EXTENDING THE LIFESPAN OF EXISTING BRIDGES THROUGH CONTROLLABLE STIFFNESS AND DAMPING DEVICES

December 2008

Richard E. Christenson

JHR 08-317 Project 06-3

This research was sponsored by the Joint Highway Research Advisory Council (JHRAC) of the University of Connecticut and the Connecticut Department of Transportation and was performed through the Connecticut Transportation Institute of the University of Connecticut.

Technical Report Documentation Page

1. Report No.	2. Government Accession No.	3. Recipient's Catalog No.
JHR 08-317	N/A	

4. Title and Subtitle	5. Report Date
Extending the Lifespan of Existing Bridges through Controllable Stiffness and Damping Devices	December 2008
	6. Performing Organization Code: N/A

7. Author(s)	8. Performing Organization Report No.
Richard E. Christenson	JHR 08-317

9. Performing Organization Name and Address	10. Work Unit No. (TRAIS)
University of Connecticut Connecticut Transportation Institute Storrs, CT 06269-5202	N/A
	11. Contract or Grant No.: N/A

12. Sponsoring Agency Name and Address	13. Type of Report and Period Covered
Connecticut Department of Transportation 280 West Street Rocky Hill, CT 06067-0207	FINAL
	14. Sponsoring Agency Code: N/A

15. Supplementary Notes

This study was conducted under the Connecticut Cooperative Highway Research Program (CCHRP, http://www.cti.uconn.edu/chwrp/index.php).

16. Abstract

This study examines the protection of highway bridges from heavy vehicle traffic induced vibrations through the use of controllable stiffness and damping devices for both structural control and structural health monitoring (SHM).

A literature review of previous structural control strategies applied to mitigate vehicle induced bridge vibration is first provided. An analytical model of an in service highway bridge under heavy vehicle truck loading is then developed and four types of ideal structural control devices are considered for analytical testing; passive stiffener, passive damper, active device, and semiactive device. The structural control performance is evaluated under various loading cases and bridge parameter values. The results show that in general the performance efficiency and robustness of the active and semiactive devices was greater than either of the passive devices. The semiactive control strategy can provide similar performance for a range of vehicle speeds and, using the same hardware, similar performance as applied to bridges with a different stiffness.

A SHM method for identifying local nonlinear damage on a highway bridge is proposed. The semiactive control strategy used to reduce bridge vibration is employed for monitoring purposes. The proposed SHM method utilizes the coherence relationship between the semiactive device input and the midspan acceleration vibration response output. An analytical study is conducted to investigate the capability of the SHM method to accurately and precisely detect damage evident as local nonlinear behavior. Results from the study demonstrate a high sensitivity of the SHM method to identify the local damage.

The results of this analytical study illustrate the benefits of controllable stiffness and damping devices for both semiactive structural control of bridge vibrations and for enhanced bridge health monitoring.

17. Key Words	18. Distribution Statement
Bridge vibration, Structural control, Structural health monitoring	No restrictions. This document is available to the public through the National Technical Information Service Springfield, Virginia 22161

19. Security Classif. (of this report)	20. Security Classif. (of this page)	21. No. of Pages	22. Price
Unclassified	Unclassified	44	N/A

Form DOT F 1700.7 (8-72) Reproduction of completed page authorized

ACKNOWLEDGEMENTS

This research was sponsored by the Joint Highway Research Advisory Council of the University of Connecticut and the Connecticut Department of Transportation through Project 06-3. The authors would like to acknowledge the generosity of Prof. John DeWolf for providing measured strain data from the Cromwell Bridge to validate the bridge model developed in this work.

SI* (MODERN METRIC) CONVERSION FACTORS

APPROXIMATE CONVERSIONS TO SI UNITS

SYMBOL	WHEN YOU KNOW	MULTIPLY BY	TO FIND	SYMBOL
		LENGTH		
in	inches	25.4	millimeters	mm
ft	feet	0.305	meters	m
yd	yards	0.914	meters	m
mi	miles	1.61	kilometers	km
		AREA		
in^2	square inches	645.2	square millimeters	mm^2
ft^2	square feet	0.093	square meters	m^2
yd^2	square yard	0.836	square meters	m^2
ac	acres	0.405	hectares	ha
mi^2	square miles	2.59	square kilometers	km^2
		VOLUME		
fl oz	fluid ounces	29.57	milliliters	mL
gal	gallons	3.785	liters	L
ft^3	cubic feet	0.028	cubic meters	m^3
yd^3	cubic yards	0.765	cubic meters	m^3
	NOTE: volumes greater than 1000 L shall be shown in m^3			
		MASS		
oz	ounces	28.35	grams	g
lb	pounds	0.454	kilograms	kg
T	short tons (2000 lb)	0.907	megagrams (or "metric ton")	Mg (or "t")
		TEMPERATURE (exact degrees)		
°F	Fahrenheit	5 (F-32)/9 or (F-32)/1.8	Celsius	°C
		ILLUMINATION		
fc	foot-candles	10.76	lux	lx
fl	foot-Lamberts	3.426	$candela/m^2$	cd/m^2
		FORCE and PRESSURE or STRESS		
lbf	poundforce	4.45	newtons	N
lbf/in^2	poundforce per square inch	6.89	kilopascals	kPa

APPROXIMATE CONVERSIONS FROM SI UNITS

SYMBOL	WHEN YOU KNOW	MULTIPLY BY	TO FIND	SYMBOL
		LENGTH		
mm	millimeters	0.039	inches	in
m	meters	3.28	feet	ft
m	meters	1.09	yards	yd
km	kilometers	0.621	miles	mi
		AREA		
mm^2	square millimeters	0.0016	square inches	in^2
m^2	square meters	10.764	square feet	ft^2
m^2	square meters	1.195	square yards	yd^2
ha	hectares	2.47	acres	ac
km^2	square kilometers	0.386	square miles	mi^2
		VOLUME		
mL	milliliters	0.034	fluid ounces	fl oz
L	liters	0.264	gallons	gal
m^3	cubic meters	35.314	cubic feet	ft^3
m^3	cubic meters	1.307	cubic yards	yd^3
		MASS		
g	grams	0.035	ounces	oz
kg	kilograms	2.202	pounds	lb
Mg (or "t")	megagrams (or "metric ton")	1.103	short tons (2000 lb)	T
		TEMPERATURE (exact degrees)		
°C	Celsius	1.8C+32	Fahrenheit	°F
		ILLUMINATION		
lx	lux	0.0929	foot-candles	fc
cd/m^2	$candela/m^2$	0.2919	foot-Lamberts	fl
		FORCE and PRESSURE or STRESS		
N	newtons	0.225	poundforce	lbf
kPa	kilopascals	0.145	poundforce per square inch	lbf/in^2

*SI is the symbol for the International System of Units. Appropriate rounding should be made to comply with Section 4 of ASTM E380.
(Revised March 2003)

TABLE OF CONTENTS

Technical Report Documentation Page ii
Acknowledgments iii
Modern Metric Conversion Factors iv
Table of Contents v
List of Figures vi
1. Introduction 1
2. Examining the Effectiveness of Semiactive Structural Control to Reduce Traffic Induced Bridge Vibration 1
2.1 Motivation for Structural Control 2
2.2 Literature Review of Structural Control for Traffic Induced Bridge Vibration 4
2.3 Highway Bridge Model with Truck Loading and Control Device 8
2.3.1 Galerkin Method Formulation of Highway Bridge Model 9
2.3.2 Truck Force Description 12
2.3.3 Control Force Description 12
2.4 Highway Bridge Model Validation 14
2.5 Mechanical Amplifying Device 15
2.6 Structural Control Strategies for Truck Excited Highway Bridge 16
2.6.1 Passive Control Strategies 16
2.6.2 Active Control Strategy 16
2.6.3 Semiactive Control Strategy 17
2.6.4 Performance of Optimal Control Strategies 17
2.7 Robust Performance of Structural Control Strategies 20
2.8 Conclusions on Structural Control to Reduce Traffic Induced Bridge Vibration 22
3. Development of a Coherence-Based Structural Health Monitoring Method for Semiactive Controlled Structures 23
3.1 Literature Review of Structural Health Monitoring 23
3.2 Proposed Coherence-Based Structural Health Monitoring Method 25
3.2.1 Results for the Undamaged Structure 28
3.3 Simulating Local Bridge Damage 31
3.4 Structural Health Monitoring Procedure and Results 32
3.5 Conclusions on SHM using Semiactive Control Devices 33
4. References 35

LIST OF FIGURES

Figure 1: Histogram displaying the number of in service bridges built organized by bridge age and by percentage of current highway bridges deemed structurally deficient by age. 2
Figure 2: Elevation View of Cromwell Bridge 8
Figure 3: Cromwell Bridge Cross Section 9
Figure 4: Fundamentals of Device Configuration with Bridge 12
Figure 5: The forces and moments associated with the device and the vertical force couples representing the device force in the analytical model 14
Figure 6: Known weight truck driven over Cromwell Bridge during experimental testing 14
Figure 7: Comparison of strain data between actual testing and model 15
Figure 8: Scissor-Jack Amplifying Device Implemented into Bridge System 15
Figure 9: Active Performance 18
Figure 10: Semiactive Performance 18
Figure 11: Passive Stiffener Performance 19
Figure 12: Passive Damper Performance 19
Figure 13: Control device performance summarized over a range of truck load speeds 21
Figure 14: Control device performance summarized over a range bridge lengths 22
Figure 15: Displacement Time History without Damage 27
Figure 16: Strain Time History without Damage 27
Figure 17: Damper Force Time History without Damage 28
Figure 18: Auto Spectral Density Function: Semiactive Device Force 29
Figure 19: Auto Spectral Density Function: Midspan Acceleration Vibration Response 29
Figure 20: Coherence Function: Damper Force Input and Midspan Acceleration Vibration Response Output 30
Figure 21: SHM Procedure: Comparing Reference State and Damage State utilizing Coherence Relation between Semiactive Device Input and Midspan Acceleration Vibration Response Output 33
Figure 22: Auto Spectral Density Function: Midspan Acceleration Vibration Response Output with Damage 33

1. Introduction

There exists a current need in our nation to address the deteriorating integrity of our infrastructure. Highway bridges in particular are continuously exceeding their design life and are increasingly being classified as structurally deficient. In 2006 over 74,000 (12%) of the total bridges in the U.S. were categorized as structurally deficient; meaning there is an eminent need for repair, rehabilitation, or reconstruction of the structure. This work attends to these particular concerns by proposing time and cost effective methods for extending the lifespan of highway bridges through controllable stiffness and damping devices. These topics are explored in the work presented through analytical and experimental research including: an analytical study on the use of various structural control strategies to mitigate heavy vehicle traffic induced highway bridge vibrations, an experimental verification of the performance of a semiactive control device to reduce vehicle induced highway bridge vibration through real-time hybrid simulation, and an analytical study which develops and evaluates a structural health monitoring method for identifying local nonlinear damage on a highway bridge.

The first topic examined in this work is use of structural control strategies to reduce heavy vehicle traffic induced highway bridge vibrations. Passive, active, and semiactive structural control strategies are each considered; but primary focus is afforded to semiactive control. A brief background on previous structural control strategies applied to mitigate bridge vibration is covered. Four types of ideal structural control devices are designed for analytical testing; passive stiffener, passive damper, active device, and semiactive device. The performance of the four structural control devices is evaluated under various loading cases and bridge parameter values.

The second topic explored in this work is the development and evaluation of a structural health monitoring procedure for identifying local nonlinear damage on a highway bridge. A semiactive control strategy is described and the device is employed to excite the highway bridge with a random white noise command for monitoring purposes. The proposed SHM method employs the coherence relationship between the semiactive device input and vibration response midspan acceleration output. An analytical study is conducted to investigate the SHM method's ability to accurately and precisely detect local nonlinear damage.

2. Examining the Effectiveness of Semiactive Structural Control to Reduce Traffic Induced Bridge Vibration

This study examines reducing heavy vehicle traffic induced highway bridge vibrations through the use of structural control strategies. Passive, active, and semiactive structural control strategies are each examined; but primary focus is afforded to semiactive control. A brief background on previous structural control strategies applied to mitigate vehicle induced bridge vibration is covered. For this work an analytical model of an in service highway bridge under heavy vehicle truck loading is developed. Four types of ideal structural control devices are considered for analytical testing; passive stiffener, passive damper, active device, and semiactive device. The structural control device is integrated into the bridge system and the performance of the four structural control devices are evaluated under various loading cases and bridge parameter values. The results show that in general the performance efficiency and robustness of the active and semiactive devices was greater than either of the passive devices. Beyond the

performance based criterion the semiactive control device awards additional benefits by offering multi-hazard protection and multi-bridge application and demonstrates beneficial intrinsic characteristics. As such the semiactive control device is selected as the most attractive control strategy for mitigating heavy vehicle induced highway bridge vibrations.

2.1 Motivation for Structural Control

Highway bridges are a significant and critical component of the civil infrastructure in the United States. There are nearly 600,000 public highway bridges in the United States (Kirk and Mallet, 2007), about 90% of all personal travel and 80% of all freight travel is accommodated on highways traveling over these bridges (Friedland and Small, 2003). Figure 1 shows a histogram of the age of bridges in the U.S. along with the percentage of bridges classified in 2006 as either structurally deficient and/or functionally obsolete by the Federal Highway Administration (FHWA). The large number of bridges built more than 40 years ago is compounded by the fact that traditionally bridges were designed with a theoretical 50 year design life (Friedland and Small, 2003). In 2006 over 74,000 (12%) of the total bridges in the U.S. were categorized as structurally deficient; meaning there is an eminent need for repair, rehabilitation, or reconstruction (Kirk and Mallet, 2007, Friedland and Small, 2003). Observed in Figure 1, approximately 1.5% of the bridges built in the past 20 years are considered structurally deficient, compared to the 21% of bridges built between 50 to 70 years ago classified as structurally deficient. The percentage of structurally deficient bridges increases exponentially with age, reflecting the fact that the design life of many bridge structures is being exceeded. According to the trends observed in Figure 1, the problem of structurally deficient and/or functionally obsolete bridges will increase over the next few decades.

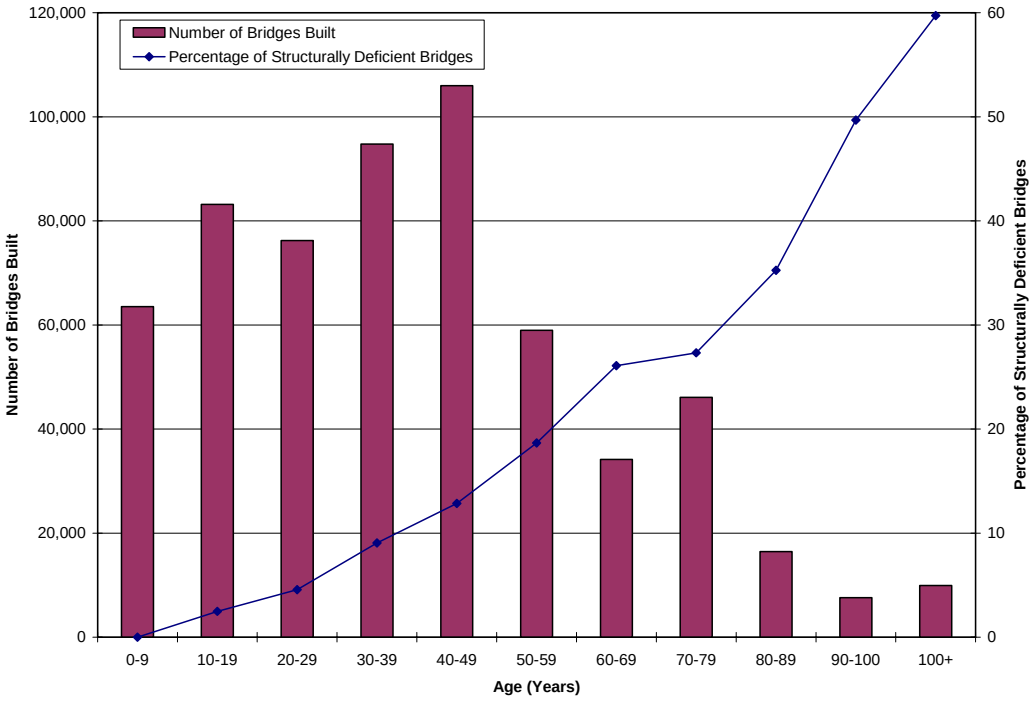

Figure 1: Histogram displaying the number of in service bridges built organized by bridge age and by percentage of current highway bridges deemed structurally deficient by age.

These statistics on the condition of the nation's highway bridges validate the sense of urgency to fix the nation's infrastructure. The U.S. Department of Transportation (DOT) estimates it would cost a total of $65.3 billion to repair and retrofit the nation's structurally deficient bridges (Kirk and Mallet, 2007). The total does not include the cost of replacing existing bridges, which would greatly increase the estimate (Kirk and Mallet, 2007). Replacing deficient bridges is an extremely time and cost consuming task and is not, in general, a realistic option. As such, addressing structural deficiencies of bridges safely, economically, and time efficiently so as to increase the safe-life and prolong replacement is of great importance to bridge owners and the public as a whole.

The life span of a bridge, which structurally is governed by fatigue caused by truck traffic, is often described in terms of fatigue life. The fatigue evaluation of steel bridges is typically categorized as either load-induced or distortion-induced damage. Load-induced fatigue arises from in-plane stresses in the steel plates that make up bridge member cross sections (AASHTO LRFR 2003). There are two levels of load-induced fatigue evaluation; the infinite-life check and the finite-life calculation. A fatigue prone detail of a steel bridge that is found to have an infinite life, i.e. passes the infinite-life check, is found to have an infinite-life because it experiences a maximum stress range which is less than or equal to the constant amplitude fatigue threshold. The infinite life check formula can be found in the AASHTO Manual for Condition Evaluation and LRFR of Highway Bridges. The maximum stress range for the fatigue prone detail can either be numerically calculated or experimentally measured for the bridge in question, with appropriate evaluation constants applied. The constant amplitude fatigue threshold for the fatigue prone detail can be found in the AASHTO LRFD Bridge Design Specifications.

A bridge which does not pass the infinite-life check is said to have a finite-life. The finite-life of a steel bridge is calculated using the equation developed in NCHRP Report 299 and adopted by the AASHTO Manual for Condition Evaluation and LRFR of Highway Bridges (AASHTO LRFR 2003)

$$Y = \frac{R_R A}{365 n (ADDT_{SL})(\Delta f_{eff}{}^3)} \tag{1}$$

where Y is the total finite fatigue life (in years), R_R is the resistance factor specified for evaluation, minimum, or mean fatigue life, A is the detail category constant, n is the estimated number of stress range cycles per truck passage, $ADDT_{SL}$ is the average number of trucks per day in a single lane averaged over the fatigue life, and Δf_{eff} is the effective stress range. The values for R_R and n are specified in the AASHTO Manual for Condition Evaluation and LRFR of Highway Bridges. The values for A and $ADDT_{SL}$ are given in the AASHTO LRFD Bridge Design Specifications. The maximum effective stress range, Δf_{eff}, is calculated numerically or through monitoring.

The life span, or total finite fatigue life, of a bridge can be increased in Equation (1) by: changing the bridge details; decreasing the number of trucks traveling over the bridge; and/or reducing the dynamic response of the bridge, reducing peak stresses, and thus the effective stress range. Changing bridge details can be a tedious and costly process for existing bridges. Decreasing the number of trucks may not be feasible within the transportation network. Reducing the dynamic response of truck traffic appears to be a particularly promising means by which to increase the safe life of an existing highway bridge because the fatigue life is inversely proportional to the cube of the stress range.

Reducing the dynamic response and resulting peak stresses can be accomplished by reducing vehicle weights, modifying the structural system itself, or integrating a structural control device. Eighty percent of the freight traffic in the US is on highways and travels over highway bridges. These vehicles play an important role in commerce for the nation (Friedland and Small, 2003). The increased efficiency of larger payloads makes reducing vehicle weights a less desirable option. Retrofitting a bridge to modify the structural system is often a time and cost consuming measure and while traditionally this is the method chosen to increase bridge safe life, there may exist more efficient methods through structural control.

Structural control shows great potential for reducing vibrations in various civil structures. There are three primary classes of structural control devices: passive, active, and semiactive (Spencer and Sain, 1997). Passive devices, such as viscous dampers, require no external power to operate however their parameters are fixed which quite often results in limited performance. Active control devices, such as hydraulic actuators, are fully controllable providing high performance however they can require significant power to operate and can raise issues of stability. Semiactive devices include controllable stiffness and damping devices which are used to produce dissipative and conservative control forces. Semiactive control devices require little energy to operate, are controllable in real time, and are inherently stable (Spencer and Sain, 1997). Semiactive control devices offer the reliability associated with passive control devices while maintaining the versatility associated with active control devices. Semiactive devices typically require a low power supply compared to active control devices (Spencer and Nagarajaiah, 2003) (e.g. a 200 kN Magneto-Rheological fluid damper can operate with a 20 volt power supply). Structural control, in particular semiactive structural control, appears to be well suited to increase the safe life of existing highway bridges.

This paper provides a background on previous structural control strategies applied to reduce vehicle induced bridge vibration. Following, an analytical model of an in service highway bridge system with truck loading is defined. The combined bridge-truck model is validated using actual measured bridge data from a permanently monitored highway bridge in Connecticut. Ideal passive, active and semiactive control strategies are proposed for the bridge model with traffic loading. The performance of the semiactive control device, compared to uncontrolled, passive and active control, at reducing heavy vehicle induced vibrations for a range of truck loading and bridge properties is examined.

2.2 Literature Review of Structural Control for Traffic Induced Bridge Vibration

In recent years utilizing structural control devices as a method for reducing vibrations of structures has received significant attention. During the past four decades researchers have worked to turn the concepts of structural control into a feasible technology for civil structures (Spencer and Nagarajaiah, 2003).

The use of structural control devices to mitigate the vibration of a structure has been investigated largely for seismic and wind induced vibration in buildings and bridges. Analytical and experimental research has lead to the full scale implementation of structural control for civil structures. Structural control devices, including passive, active and semiactive, have been implemented on buildings and bridges all over the world. Research and implementation have demonstrated the benefits and rewards that structural control devices offer; most apparent being that these devices allow for safer and more economical structures.

Over the past decade various research has examined the mitigation of traffic induced vertical bridge vibration. Unlike lateral motion of bridges involving seismic and wind excitations, the vertical vibrations are typically attributed to vertical forces traveling along the

length of the bridge. To date, researchers have primarily investigated pedestrian, train, and vehicle induced vibrations. Structural control devices including all three classes; passive, active, and semiactive, have been investigated as a means for mitigating vertical vibrations induced by time varying vertical loads. These studies are discussed in what follows.

The implementation of passive devices including tuned liquid column dampers (TLCDs) and tuned mass dampers (TMDs) has been investigated for reducing vibrations arising from pedestrian, train, and truck loading of bridges. The control of pedestrian induced vibrations on long-span bridges using TLCDs was explored by Reiterer and Ziegler (2005). In an analytical study preformed by Reiterer and Zeigler it was found that by utilizing TLCDs vertical vibrations could effectively be reduced. The control of train induced vibrations using passive TMDs has also been investigated. An analytical study conducted by Kwon et al. (1998) investigated the use of a TMD to control vertical vibrations under moving train loads. In this study the bridge was modeled as an Euler-Bernoulli beam excited by a high-speed train and a TMD was placed at the midspan of the bridge. Results from the study showed that by employing the TMD the maximum vertical displacements generated by the high-speed train were effectively reduced by 21% and free vibration of the bridge quickly died out. Klasztorny (2001) also examined the effects of using a TMD to reduce bridge responses. More specifically, Klasztorny examined the effectiveness of a TMD at reducing resonant responses of a bridge subjected to a superfast passenger train. Klasztorny analytically examined several bridges subject to critical train speeds and the effectiveness of the TMD designed specifically for each bridge at reducing vibrations. Klasztomy's research shows midspan displacements and stresses were shown to be reduced by as much as 60%. Karoumi (2000) investigated truck traffic induced vibrations of cable-stayed bridges. Karoumi describes a method for modeling the bridge and truck which includes a nonlinear finite element model (FEM) of the bridge using beam and cable elements and a 2 degree of freedom (DOF) model for the truck. An analytical analysis of the cable-stayed bridge model subjected to the truck model with a TMD located at the center of the bridge and tuned to the first bending mode of vibration is presented by Karoumi. The results of the analytical study indicate that the TMD is not effective at reducing the maximum dynamic response during forced vibration but is very effective at reducing the dynamic response during free vibration. In general results presented for TLCD and TMD passive control devices to reduce vertical bridge vibrations have shown a positive trend. However, there are several drawbacks to these devices which should not be ignored. The drawbacks include: the device weight and fixed parameters inherent of passive control devices. The added weight of a TLCD or TMD on a bridge effectively reduces the capacity of the bridge. The fixed parameters of a passive device mean that the device is not controllable in real-time. In addition, the fixed parameters of the device are exclusively determined for each application in order to assure effectiveness; meaning a new device design must be obtained for each individual bridge employing a control device of this nature.

Another type of passive device has been considered for reducing vertical bridge vibrations is a fluid viscous damper (FVD). Museros and Martinez-Rodrigo (2007) investigated the use of linear FVDs to mitigate vertical bridge vibrations of simply supported beam bridges. Museros and Martinez-Rodrigo explored the use of a damping system consisting of a simply supported auxiliary beam located below the bridge, parallel in direction, with FVDs linking the beam and bridge at several locations. The focus for the design of the control system in their research was to mitigate flexural vibrations of the bridge produced by railway traffic. The analytical research presented by Museros and Martinez-Rodrigo demonstrated that the vertical vibrations of the simply supported beam bridge could drastically be reduced at resonant excitations using the developed control system. Graphical results from the research show a reduction in bridge:

accelerations, displacements, stresses, and end reactions. Two bridge lengths with ideally designed control parameters specific to each bridge were considered in the research; for one particular case maximum midspan accelerations were reduced by 80.9% and maximum midspan displacements were reduced by 58.8%. Similar to the passive devices mentioned earlier in this paper, a drawback inherent of passive control devices exists. The detail that passive control parameters must be specifically designed for each individual structure they are being applied to and loading they are subject to. This characteristic makes the application of these devices to different and multiple structures very time consuming, alluding to the fact that a device of this nature would have difficulty becoming widespread in application.

Utilizing active control devices to mitigate vertical bridge vibrations has also been investigated. The idea of using active control has been intensely addressed by DeBrunner et al. (2001, 2003, 2004). DeBrunner et al. (2003) investigated reducing bridge vibrations induced by heavy vehicle traffic. DeBrunner et al. propose the use of a black box identification method and an adaptive vibration control technique with feed forward and feedback active control; the control system developed is called the Intelligent Vehicle/Bridge System (IVBS). The IVBS combines the use of sensors, antennas, DSP controllers, and active control actuators to mitigate bridge vibrations. For the IVBS described by DeBrunner et al. (2003, 2004) the active control actuators are installed on the trucks. Analytical results presented by DeBrunner et al. report a very efficient reduction in bridge vibrations. Like passive control devices, active control devices have several drawbacks in bridge application intrinsic in their makeup. The drawbacks are that active control devices require significant power to operate and have the potential to become unstable.

Mitigating vertical bridge vibrations by employing semiactive control devices has received significant attention from researchers. The research in this control realm focuses on vehicle traffic induced bridge vibrations (Patten et al., 1996, 1996, 1997, 1998, 1998, 1999, 1999, Zeng et al., 2000, Sammartino et al.,1999). Patten et al. (1996) designed and constructed a semiactive control device which was experimentally tested. Patten et al. modeled the bridge considered in the study as an Euler-Bernoulli beam and the truck as a 2 DOF system; these models were used to design the controller for the bridge. Patten et al (1996) designed a semiactive hydraulic actuator which uses feedback control based on either strain-gage or accelerometer readings from the bridge. A single-lane bridge was constructed to experimentally investigate the effectiveness of the semiactive vibration absorber. The semiactive vibration absorber was shown to provide a significant reduction of vertical bridge vibrations; deflections were reduced by more than 70%. The semiactive vibration absorber was also tested as a fixed damper, i.e. passive control device; the deflection reduction was more than 30% greater utilizing the semiactive vibration absorber compared to the passive vibration absorber.

Additional research into the area of semiactive control devices for traffic induced vibration mitigation was preformed by Patten et al. (1999). Patten et al. present a semiactive control system; called the Smart Bridge Dampers (SBD) system, which employs a semiactive vibration absorber as the controllable element. The SBD system includes a hydraulic actuator with a motor controlled valve; the motor controlled valve is regulated to provide appropriate amounts of stiffness and damping to the bridge in order to minimize bridge vibrations. Analytical simulations indicated that by using the SBD system maximum stresses were reduced by as much as 65% and the useful service life of the bridge was extended by approximately 65 years (Patten et al., 1999).

Further experimental research was preformed by Patten et al (1997) in the first, and only to date, full scale implementation of a semiactive control device onto a highway bridge for the purpose of reducing vehicle traffic induced vibrations. The semiactive vibration absorbers (SAVA) system was installed on the Walnut Creek Bridge on Interstate 35 in Oklahoma, installation of the SAVA system was completed in October of 1996. Initial results from field tests suggested that the SAVA system was capable of increasing the safe life of the Walnut Creek Bridge by several decades.

Further research and data collection presented by Patten et al. (1999) includes the employment of intelligent stiffeners for bridges (ISB) in the SAVA system, referred to as SAVA I. ISB are semiactive control devices which use 12 volt batteries and are equipped with adjustable hydraulic links used to regulate the amount of stiffness and damping provided to the bridge. The design of the IBS controllers was based on a FEM developed from modal testing and model reductions and a multi-DOF truck model. The IBS controllers were implemented into the SAVA I system and testing was conducted for 22 months. The SAVA I system employs a full-state control algorithm based on Lyapunov stability theory in order to control the ISB. Patten et al. (1999) concluded that the SAVA I system equipped with IBS was able to significantly reduce the maximum stresses in the girders of the Walnut Creek Bridge, resulting from a reduction in the displacements and velocities of the girders, and increase the safe life of the bridge by about 50 years. Further research was conducted on the Walnut Creek Bridge by Zeng et al. (2000) where a bi-state Lyapunov control algorithm employing only 3 sensors, where all sensors are installed directly onto the semiactive actuator, was considered. This second ISB prototype was installed on the Walnut Creek Bridge in 1998 and is the major element which differentiates this system, SAVA II, from SAVA I. Simulations indicated that the SAVA II system exhibits favorable behavior for vibration mitigation. Field tests comparing SAVA II, bi-state control algorithm, to SAVA I, full-state control algorithm, found that SAVA I reduced peak stresses by 40% and SAVA II reduced peak stresses by 33%. Zeng et al. note that although the SAVA II system provides less stress reduction, it is much more cost efficient and practical for use on a large structure.

Sammartino et al. (1999) have also proposed a method for minimizing the structural vibration of a vehicle and bridge system utilizing semiactive control. Sammartino et al. developed a beam bridge FEM and a multi-DOF vehicle model. The bridge model was intended to represent the Kishwaukee Bridge in Rockford Illinois; the first 3 modes of the model were validated with experimental testing data from the Kishwaukee Bridge. Analytical simulations were conducted by the Sammartino et al. exploring the effectiveness of passive and semiactive control devices applied to the vehicle and variable vehicle speeds. In general bridge deflections were reduced by a greater percent using the semiactive control as opposed to the passive control; deflections were reduced by as much as 56% using the semiactive control.

Research, analytical studies, and experimental testing reported by researchers have efficiently demonstrated that structural control devices are a feasible and promising option for reducing vertical bridge vibrations. Of the three control device types semiactive devices have shown particular promise for this type of structural application. Semiactive control devices are emerging in the forefront because they offer several advantages compared to their competitors and are capable of demonstrating robust performance. Specifically, semiactive devices benefit over passive devices in that they are controllable in real-time; passive devices are not. Semiactive devices benefit over active devices in that they require little power to operate and they do not have the potential to become unstable; active devices require a significant amount of

power to operate and have the potential to become unstable. Semiactive devices offer multi-hazard protection; more specifically this type of device affords protection from many excitations including: varying truck speeds, varying truck configurations and loads, earthquakes, wind loads, etc.; the device reduces vertical vibrations regardless of their origin. Semiactive control devices offer robust performance fostering a multi-bridge application. More explicitly identical devices can be used on many different bridges without being redesigned or altered; the physical device is not bridge specific.

To date and to the knowledge of the authors, no studies have been published on the performance of structural control over a range of truck excitations and bridge properties directly comparing passive, active, and semiactive control devices. This paper examines the performance of passive, active and semiactive control strategies applied to a typical highway bridge, considering variations in the dynamic load and bridge structure.

2.3 Highway Bridge Model with Truck Loading and Control Device

A highway bridge model with associated truck loading and control device application is developed. The bridge model is to represent a typical highway bridge and is based on an actual in service highway bridge located in Connecticut. The truck loading represents a 5 axle truck driving over the bridge at a constant velocity. The control device represents vertical supplemental control device forces applied at specified locations on the bridge.

The bridge selected for this study, the Cromwell Bridge, is located in the southbound direction of Interstate 91 (I-91) in Connecticut. The bridge is a simply supported composite, steel girder and concrete slab, bridge. The Cromwell Bridge is approximately 66 meters (215 ft) in length; with 3 simply supported spans of lengths approximately 23 meters (75 ft), 23 meters (75 ft), and 19 meters (63 ft). Expansion joints are located between each of the spans (50.8 mm (2 in)). Figure 2 shows an elevation view of the Cromwell Bridge, the span selected for modeling is indicated with a red circle.

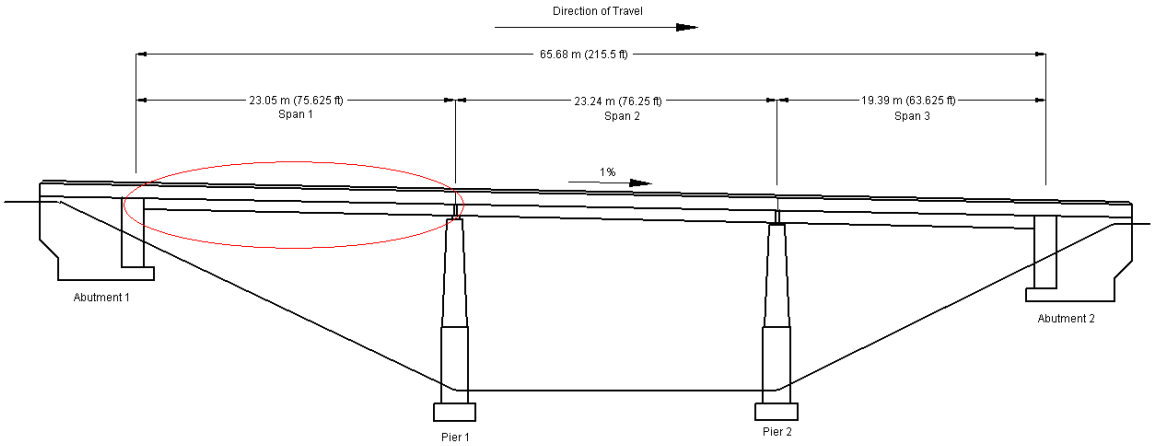

Figure 2: Elevation View of Cromwell Bridge

The width of the bridge is approximately 15.5 meters (51 ft) and carries three lanes of traffic. A view of the cross section of the bridge can be seen in Figure 3; which details the locations and specifications of the girders, diaphragms, and cover plates as well as the dimensions of the deck and side barriers.

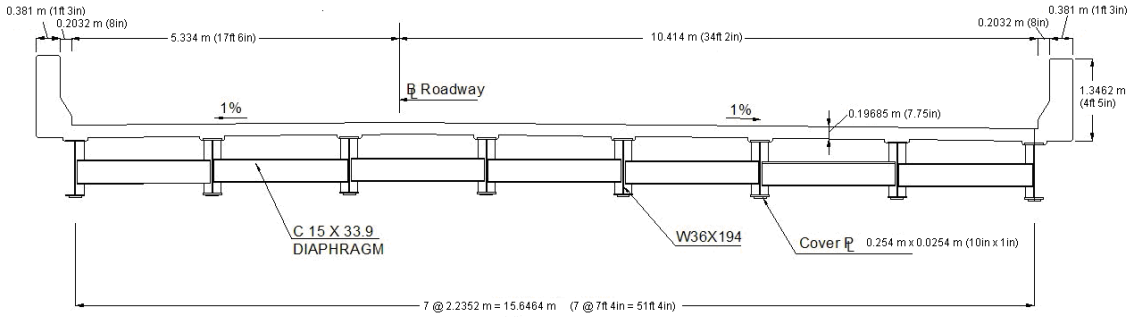

Figure 3: Cromwell Bridge Cross Section

The Cromwell Bridge is one of six bridges currently being monitored in a combined effort bridge monitoring project hosted by the University of Connecticut and the Connecticut Department of Transportation. Spans 1 and 2 of the bridge have been monitored since November 2004. In total there are 20 uniaxial strain gages installed on the bridge; 16 on span 1 and 4 on span 2. The strain gages are installed on the web of the steel W36x194 girders; either 50.8 mm (2 in) from the top of the bottom flange or 50.8 mm (2 in) from the bottom of the top flange. The monitoring system records strain data at a sampling rate of 50 Hz and with a 1με resolution. The actual strain measurements for a known truck load are used to validate the model developed in this paper.

An infinite-life check for the Cromwell Bridge was preformed by the authors using strain data collected from the bridge monitoring efforts. The calculations indicate that the maximum stress range experienced by the structure was well below the constant amplitude fatigue threshold. As such, the Cromwell Bridge has, in reality, an infinite-life. However, for this study it is assumed that the corresponding bridge model has a finite fatigue life so that reducing stresses in the bridge will translate to increased safe life.

2.3.1 Galerkin Method Formulation of Highway Bridge Model

A low order model of the bridge is sought to capture the salient features of the vertical bridge dynamics in order to better facilitate the control design and evaluation of the system. Span 1 of the Cromwell Bridge is modeled, as this span of the bridge has been the subject of a long term monitoring project since 2004 and data is available to validate the bridge model. The first span of the bridge can be assumed as its own entity because of the structural constituents, essentially pinned-roller end conditions. Span 1 of the Cromwell Bridge is modeled as a simply supported Euler-Bernoulli beam (Clough and Penzien, 1993) with pin-roller end conditions. The simplified beam model is assumed to have a constant cross-section and material properties (e.g. modulus of elasticity and mass per unit length) along its length. The inputs of the system are vertical point loads representing a vehicle traveling across the bridge and an applied control force. The vehicle loading representing a 5 axle truck traveling at a constant speed is modeled as a time and spatially varying load, $F_t(x,t)$. The control force loading represents N vertical supplemental control device forces applied at $x = x_c^j$ (where $j = 1,...,N$) on the bridge is modeled as a time varying load, $F_c(t)$. The equation of motion governing the dynamic behavior of the undamped bridge model with applied truck and damper forces is presented as the partial differential equation

$$\bar{m}\frac{\partial^2 y(x,t)}{\partial t^2} + EI\frac{\partial^4 y(x,t)}{\partial x^4} = F_t(x,t) + \sum_{j=1}^{N} F_c^j(t)\delta\left(x - x_c^j\right) \tag{2}$$

where $y(x,t)$ is the vertical displacement of the bridge; a function of both distance along the length of the bridge, x, and time, t, $\bar{m}$ is the mass per unit length of the bridge, E is the modulus of elasticity, I is the moment of inertia for the composite cross section of the bridge, and $\delta(\cdot)$ is the Dirac delta function. The $\bar{m}$, E, and I, are assumed constant along the length of the bridge. The mass per unit length, $\bar{m}$, calculated as the product of the cross section area and the appropriate material mass density, is determined to be 11.7e3 kg-m/s (1.7025 lb-sec/in^2). The modulus of elasticity, E, is selected as the modulus of elasticity of steel 2x10^8 kPa (29000 ksi). The moment of inertia, I, is calculated using classical methodology (Beer et al., 2006) taking into account effective areas for the concrete components of the cross section to be 0.156074 m^4 (3.7497x10^5 in^4).

The partial differential equation of motion for the bridge model system in Equation (2) can be written as an ordinary differential equation using a Galerkin method. The Galerkin method assumes that response of the bridge is represented by the finite series

$$y(x,t) = \sum_{i=1}^{n} \phi^i(x) q^i(t) = \Phi(x)Q(t) \tag{3}$$

where $\phi^i(x)$ is the ith trial function of the bridge, $q^i(t)$ is the ith generalized coordinate of the bridge and n is sufficiently large to ensure accuracy (n = 40 for this study). $\Phi(x)$ and $Q(t)$ are the matrix representations of the trial functions and generalized coordinates, respectively, such that $y(x,t) = \Phi(x)Q(t)$. The trial functions are based on the closed-form eigenfunctions of an Euler-Bernoulli beam with an additional shape function equal to the static deflected shape of the simply supported beam with moments applied at the location of the device connections. This static deflection shape replaces the first sinusoidal trial function. The trial functions are given as

$$\phi^i(x) = \begin{cases} AL(\alpha - 0.5)x & i = 1 \quad x \le \alpha L \\ A/2\left(x^2 - xL + \alpha^2 L^2\right) & i = 1 \quad \alpha L < x < (1-\alpha)L \\ AL(\alpha - 0.5)(L - x) & i = 1 \quad x \ge (1-\alpha)L \\ B\sin(i\pi x / L) & i = 2,3,...,n \end{cases} \tag{4}$$

where the constants A and B can be set to any value to produce a desired norm for the mode shapes, and α is the ratio of the distance from the end of the bridge to the location of the control device divided by the total length of the bridge.

Substituting Equation (3) into (2) results in

$$\bar{m}\frac{\partial^2 (\Phi(x)Q(t))}{\partial t^2} + EI\frac{\partial^4 (\Phi(x)Q(t))}{dx^4} = F_t(x,t) + \sum_{j=1}^{N} F_c^j(t)\delta\left(x - x_c^j\right) \tag{5}$$

The trial functions are invariant to time and the generalized coordinates are invariant to position; as a result Equation 5 can be rewritten as

$$\overline{m}\Phi(x)\ddot{Q}(t) + EI\Phi''''(x)\ Q(t) = F_t(x,t) + \sum_{j=1}^{N} F_c^{\,j}(t)\delta\left(x - x_c^{\,j}\right) \tag{6}$$

where $[\dot{\cdot}]$ indicates a derivative with respect to time, t, and $[']$ indicates a derivative with respect to distance along the length of the bridge, x. This equation of motion governing the dynamic behavior of the bridge model with applied truck and damper forces is next premultiplied by $\Phi^T(x)$ and integrated over the length of the bridge to get

$$M\ddot{Q}(t) + KQ(t) = \overline{F}_t(t) + \sum_{j=1}^{N} \overline{F}_c^{\,j}(t) \tag{7}$$

where $M = \overline{m}\int_0^L \Phi^T(x)\Phi(x)\partial x$, $K = EI\int_0^L \left(\Phi''^T(x)\right)\left(\Phi''(x)\right)\partial x$, $\overline{F}_t(t) = \int_0^L \Phi^T(x)F_t(x,t)\partial x$ and $\overline{F}_c^{\,j}(t) = F_c^{\,j}(t)\Phi^T(x_c^j)$. Inherent damping is added to the bridge model where the damping coefficient matrix, *C*, is

$$C = \overline{\Phi}(x)\overline{C}\overline{\Phi}(x)^{-1} \tag{8}$$

and $\overline{\Phi}(x)$ is the matrix of mode shapes obtained by solving the eigenvalue problem with *M* and *K*, $\overline{C}$ is the diagonal modal damping matrix with the *j*th diagonal term $\overline{C}_j = 2\overline{M}_j\omega_j\varsigma_j$, where $\overline{M} = \overline{\Phi}(x)^{-1}M\overline{\Phi}(x)$ (and $\overline{M}_j$ is the *j*th diagonal term), ω_j is the natural frequency of the *j*th mode, and ς_j is the damping ratio of the *j*th mode. The resulting damped equation of motion governing the dynamic behavior of the bridge is

$$M\ddot{Q}(t) + C\dot{Q}(t) + KQ(t) = \overline{F}_t(t) + \sum_{j=1}^{N} \overline{F}_c^{\,j}(t) \tag{9}$$

Of particular interest in this study is displacement of the bridge at the midspan, x_m, the strain at midspan of the bridge, and the rotation, or slope, of the bridge at the locations of the control device connection to the bridge, x_d. These physical outputs can readily be obtained from the generalized coordinates, $Q(t)$, by utilizing the relationship in Equation (3) such that

$$y(x_m,t) = \Phi(x_m)Q(t) \tag{10}$$

$$y'(x_d,t) = \frac{dy}{dx} = \Phi'(x_d)Q(t) \tag{11}$$

$$\varepsilon(x_m,t) = y''(x_m,t)d = \frac{d^2y}{dx^2}d = \Phi''(x_m)Q(t)d \tag{12}$$

where ε represents strain and d is the distance between the neutral axis of the cross section and the location where the strain is being measured.

2.3.2 Truck Force Description

The truck force vector, $F_t(x,t)$, simulates a 5 axle truck crossing the bridge at a constant speed. The force of each axle is assumed to be of constant magnitude, but its location varies with respect to time. It is represented in the model as 5 transverse point loads moving along the bridge length in time, dependent on a constant truck speed. The truck force vector is comprised of two components; a loading vector and a magnitude coefficient such that

$$F_t(x,t) = \Gamma_t(x,t)W_t. \tag{13}$$

The loading vector, Γ_t, designates the location along the length of the bridge of each of the 5 point loads at each time step, as well as the relative weight of each axle and W_t is the total weight of the truck. The loading vector varies according to the selected truck speed, $\dot{x}_t$, the relative weight of each axial, λ_k, as a percent of the total weight of the truck, W_t, and the distance between the first axle and subsequent axles, d_k. The loading vector takes the form

$$\Gamma_t(x,t) = \sum_{k=1}^{5} \lambda_k \delta\left(x + d_k - \dot{x}_t t\right). \tag{14}$$

The corresponding modal truck force in Eq. (8) is

$$\overline{F}_t(t) = \begin{cases} W_t \sum_{k=1}^{5} \lambda_k \Phi^T\left(\dot{x}_t t - d_k\right) & \text{for} \quad (x + d_k - \dot{x}_t t) \le L \\ 0 & \text{otherwise} \end{cases} \tag{15}$$

2.3.3 Control Force Description

The control force simulates the applied force of a structural control device. The control device is implemented in a configuration similar to the variable stiffness device installed on the Walnut Creek Bridge (Patten, 1997). The control device is attached to the under side of the bridge deck, in parallel with the deck using cantilever arms fixed rigidly to the underside of the bridge deck. The connections and links connecting damper to the bridge are assumed to be rigid. The schematic in Figure 4 illustrates the basic configuration of the control device integration into the bridge system. As the bridge deflects the slope of the bridge deck causes the cantilever arms to rotate, resulting in translational displacement and velocity across the control device and thus producing a force in the control device.

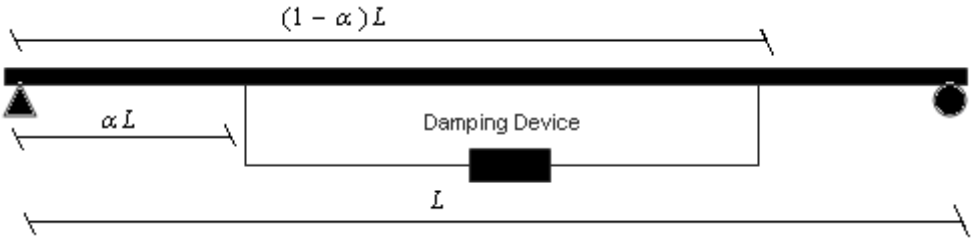

Figure 4: Fundamentals of Device Configuration with Bridge

Dominated by a first mode response, the flexural behavior of the bridge girders induces displacements and velocities across the control device. The displacement across the control device, Δ_d, is determined as a function of the bridge deformation such that difference in the curvature of the bridge at the two connection locations produces a linear displacement

$$\Delta_d = \ell\left(y'((1-\alpha)L,t) - y'(\alpha L,t)\right) \tag{16}$$

where ℓ is the length of the vertical rigid link connecting the damper to the bridge.

The force produced by the control device, $f_d(t)$, is applied to the bridge at two locations, αL and (1-α)L, and results in two applied moments on the bridge deck, equal in magnitude but opposite in direction. The control force is applied to the bridge model as two force couples at each location where the damper is connected to the bridge resulting in four transverse point loads, $F_c^j(t)$ (for j=1,2,3,4).

The force produced by the control device, $f_d(t)$, is related to the control forces applied to the bridge model, $F_c^j(t)$, as illustrated in Figure 5 and described in the following manner. The horizontal force produced by the control device results in two equal and opposite moments applied to the bridge at the connection locations [αL and (1-α)L] such that

$$M(t) = f_d(t) * \ell \tag{17}$$

where M is the moment at each connection location and ℓ is the length of the vertical rigid link connecting the damper to the bridge (i.e. lever arm length) and is assumed to have a length of 1.2192 m (48 in). The moments at each connection location are applied to the bridge model as vertical point load force couples, whereby the magnitude of the force couples relates to the moment at connection location as

$$M(t) = \left|F_c^j(t)\right| h \tag{18}$$

where h is distance between the forces in the couple and is set to $h = 0.001L$ for this study. Substituting Eq (17) into (18), solving for $F_c^j(t)$, and taking into account the assumed directions from Figure 5, results in

$$F_c^j(t) = \left(-1^{j+1}\right)(\ell/h) f_d(t) \qquad \text{for } j = 1,2,3,4 \tag{19}$$

Knowing that the locations of the force couples are $x_c^1 = \alpha L - \frac{h}{2}$, $x_c^2 = \alpha L + \frac{h}{2}$, $x_c^3 = (1-\alpha)L + \frac{h}{2}$, and $x_c^4 = (1-\alpha)L - \frac{h}{2}$, the modal control force in Eq. (8) becomes

$$\overline{F}_c(t) = \left[\Phi\left(\alpha L - \frac{h}{2}\right) - \Phi\left(\alpha L + \frac{h}{2}\right) + \Phi\left((1-\alpha)L + \frac{h}{2}\right) - \Phi\left((1-\alpha)L - \frac{h}{2}\right)\right](\ell/h) f_d(t) \tag{20}$$

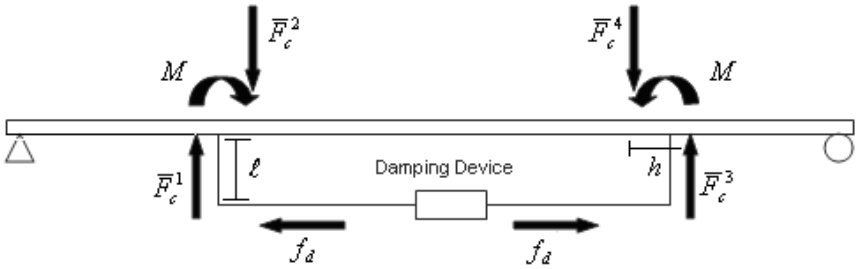

Figure 5: The forces and moments associated with the device and the vertical force couples representing the device force in the analytical model

2.4 Highway Bridge Model Validation

The numerical model of the bridge with truck loading is validated using experimental strain data from the Cromwell Bridge monitoring efforts. A known weight truck was driven across the Cromwell Bridge and corresponding strain data collected. This actual data is compared to data from the bridge model with no control force.

For the numerical model, the weight of the truck passing over the bridge is adjusted to account for two phenomenon: (i) the dynamic impact factor accounting for the vehicle dynamics induced by the roughness or irregularities on the bridge or approach surface (AASHTO LRFD Bridge Design Specifications 2004, Kwasniewski, 2006, Sammartino, 1999); and (ii) the distribution of the load across the width of the bridge, accounting for the fact that for the actual collected strain data the truck passed over the bridge in the far right lane and each girder carried an unequal portion of the trucks weight (AASHTO LRFD Bridge Design Specifications 2004, Cardini , 2007). The amplification factor accounting for both of these phenomena is set to 2.0 so that the peak strain value in the model closely matches the measured peak strain for the truck crossing. For simplification the amplification factor is held constant for all simulations. Figure 6 shows the specifications of the known weight truck. The total weight of the truck is W_t = 275.078 kN (61.84 kips). The relative weight of each axial is $\lambda_1 = 0.1727$, $\lambda_2 = 0.2222$, $\lambda_3 = 0.2144$, $\lambda_4 = 0.2044$, and $\lambda_5 = 0.1863$. The distance between the first axle and subsequent axles, $d_1 = 0$, d_2 = 5.31 m (17.42 ft), $d_3 = 6.63$ m (21.75 ft), $d_4 = 15.70$ m (51.50 ft), and $d_5 = 17.02$ m (55.83 ft). The truck is assumed to travel over the bridge at a constant velocity of 29.0576 m/sec (95.33 ft/sec, 65 mph).

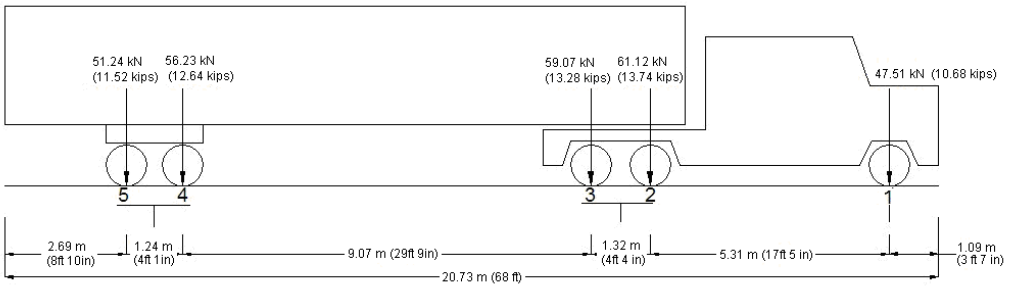

Figure 6: Known weight truck driven over Cromwell Bridge during experimental testing

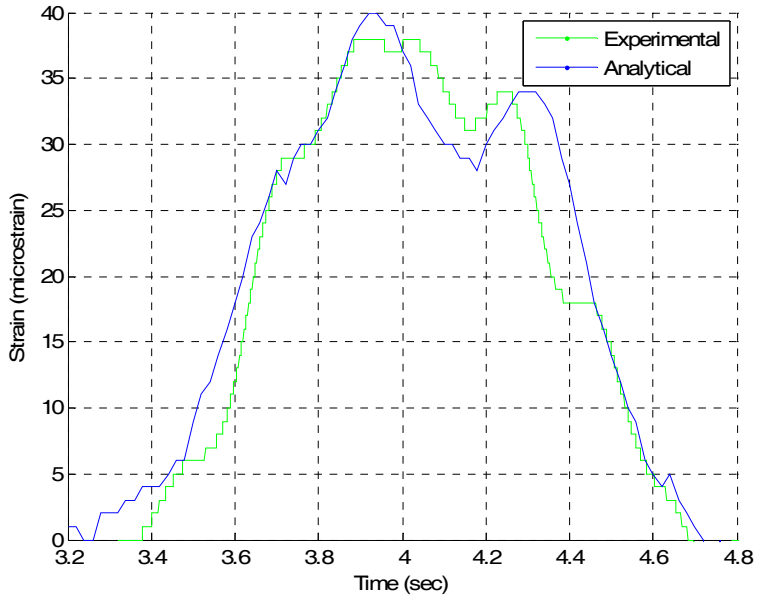

Figure 7: Comparison of strain data between actual testing and model

Figure 7 provides a comparison of the strain data between the actual testing and the results of the numerical model. The basic shape and local peak values of strain data match well between the model and actual data. The model is able to capture the critical and fundamental behavior of the Cromwell Bridge and is thus used for conducting further investigation.

2.5 Mechanical Amplifying Device

The displacement and velocity generated by the flexural behavior of the bridge girder are increased using a mechanical amplifying device. The amplification factor, γ, is selected at a value of 5.0. This degree of magnification could be achieved, for example, by using a scissor-jack-damper system (Sigaher and Constantinou, 2003). The possible integration of the scissor jack device into the bridge system is illustrated in Figure 8. This particular configuration is desirable as both the displacement across the control device and the device force are amplified by this factor.

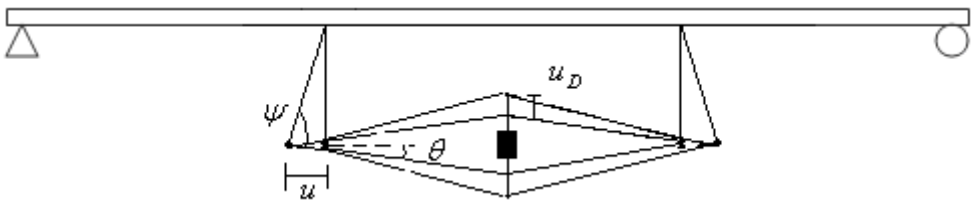

Figure 8: Scissor-Jack Amplifying Device Implemented into Bridge System

2.6 Structural Control Strategies for Truck Excited Highway Bridge

While the focus of this paper is the application of semiactive control to the highway bridge, passive and active control strategies are also considered for comparison.

2.6.1 Passive Control Strategies

Two ideal passive control devices are considered; a viscous damping device and a stiffness device. The damping device provides a control force which results from relative velocities across the control device as

$$f_d(t) = \gamma^2 c_d \dot{\Delta}_d \tag{21}$$

The stiffness device provides a control force which results from relative displacements across the control device as

$$f_d(t) = \gamma^2 k_d \Delta_d \tag{22}$$

2.6.2 Active Control Strategy

The active control strategy employs a linear-quadratic state-feedback regulator with output (y) weighting (LQRY) controller and assumes an ideal device that can produce any desired force and possesses no device dynamics.

Equations (8)-(11) can be rewritten as a state space representation of the bridge system with truck and control device loading where

$$\begin{aligned} \dot{z}(t) &= Az(t) + B_t \overline{F}_t(t) + B_d f_d(t) \\ y(x_m, t) &= Cz(t) \end{aligned} \tag{23}$$

where $z(t) = \begin{bmatrix} Q(t) & \dot{Q}(t) \end{bmatrix}$ are the states of the system, and A, B_t, B_d, C are the systems matrix coefficients where $A = \begin{bmatrix} 0 & I \\ -M^{-1}K & -M^{-1}C \end{bmatrix}$, $B_t = B_d = \begin{bmatrix} 0 \\ M^{-1} \end{bmatrix}$, and $C = \begin{bmatrix} \Phi(x_m) & 0 \\ -\Phi(x_m)M^{-1}K & -\Phi(x_m)M^{-1}C \end{bmatrix}$.

The LQRY active control strategy operates using state-feedback control, regulated by the state-feedback gain matrix K_{lqr}. The corresponding active control force is

$$f_d(t) = -K_{lqr} z(t) \tag{24}$$

where for this study it is assumed the states are known. In practice the states can be estimated with a state observer. The state-feedback gain matrix, K_{lqr}, is selected to minimize the quadratic cost function

$$J(u) = \lim_{\tau \to \infty} \frac{1}{\tau} E\left[\int_0^\tau \{(Cz(t))^T Q_{lqr} (Cz(t)) + f_d(t)^T R_{lqr} f_d(t)\} dt \right] \tag{25}$$

Simplified as: $$J(u) = \int_0^\infty (y^T Q_{lqr} y + R_{lqr} f_d(t)^2) dt \quad (26)$$

where $y(x_m, t) = \Phi(x_m) Q(t)$. The full state-feedback gain matrix K_{lqr} is equivalent to

$$K_{lqr} = R_{lqr}^{-1} B_d^T P \quad (27)$$

and P is determined by solving the Riccati equation

$$0 = PA + A^T P - P B_d R_{lqr}^{-1} B_d^T P + \widetilde{Q}_{lqr} \quad (28)$$

where $\widetilde{Q}_{lqr} = C^T Q_{lqr} C$.

For this work a Matlab toolbox function *lqry.m* was used to calculate K_{lqr}. The optimal design of the state-feedback control is accomplished by selecting values for the output weighting matrices, Q_{lqr} and R_{lqr}.

2.6.3 Semiactive Control Strategy

The semiactive control strategy is designed as a clipped optimal controller such that the semiactive device produces only the dissipative forces of a primary controller. The primary controller used is the same as that used for the active control strategy. The resulting ideal semiactive control force is

$$f_d(t) = \begin{cases} -K_{lqr} z(t) & -K_{lqr} z(t) \dot{\Delta}_d < 0 \\ 0 & otherwise \end{cases} \quad (29)$$

Additionally, the semiactive device is implemented with a rate limiter; the rate limiter restricts the slope of the device force. Because of device dynamics, the semiactive control device is not capable of instantaneously altering the force it is producing, and is thus limited to some specified rate for which the force magnitude can be changed per each time step. The rate limiter for this study is selected to have a value of 1.5e5.

2.6.4 Performance of Optimal Control Strategies

The optimal control strategy for each device is achieved by selecting a maximum force the controllers are permitted to produce. The control device parameters, c_d, k_d, $Q_{lqr,}$ and R_{lqr} are established to accomplish the maximum device force for each control strategy. The maximum device force for this study was selected as the force value realized by the active controller when reducing peak midspan displacement by 50%. The value was determined to be 124.55 kN (28 kips).

The device parameters for the passive damper and stiffener, c_d and k_d, are physical quantities which can be changed only by physically altering the device. Alternatively, for the active and semiactive devices the device parameters, $Q_{lqr,}$ and $R_{lqr,}$ are not physical values; they are numerical, housed within the control algorithm of the device. The physical design of each control device is constant for the simulations. The design is determined from the original parameters of the Cromwell Bridge subject to the known weight truck traveling at the speed limit

with a peak force limitation of 124.55 kN (28 kips). The midspan displacement time histories for each control device operating with optimal control design parameters are displayed in Figures 9 through 12. These simulations were run using 40 shape functions; which included one static deflection and 39 mode shapes. For each simulation: the original parameters of the Cromwell Bridge were considered, the control device attachments were located at $\alpha = 0.2$, a scissor magnification factor of 5.0 was utilized, and the truck velocity was 29.06m/s (95.33ft/s, 65 mph).

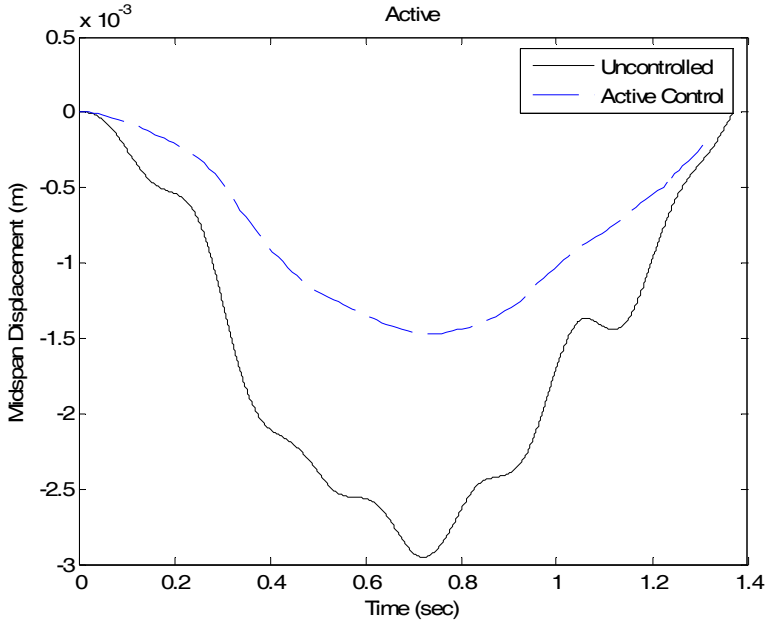

Figure 9: Active Performance

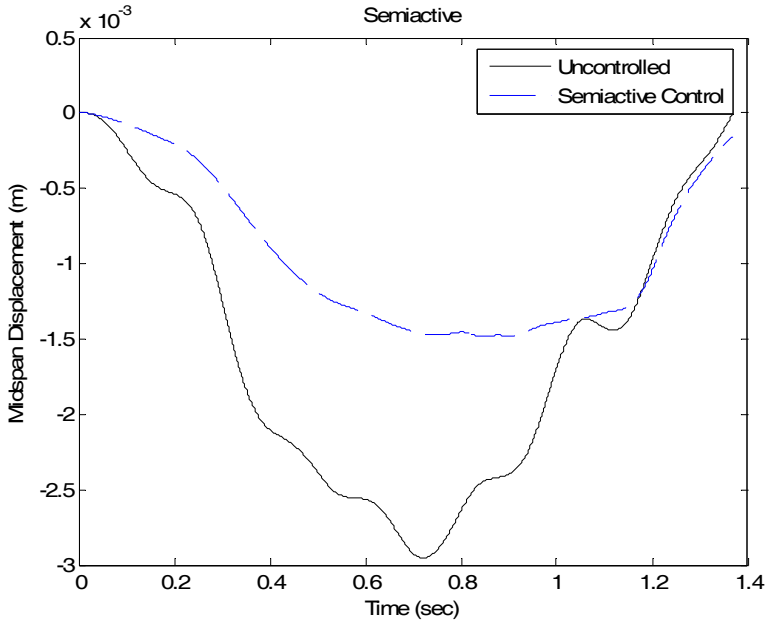

Figure 10: Semiactive Performance

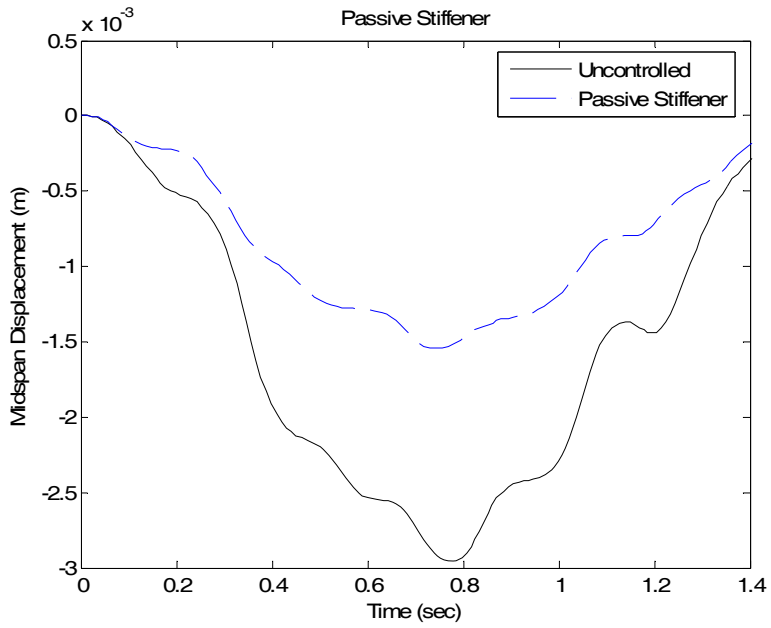

Figure 11: Passive Stiffener Performance

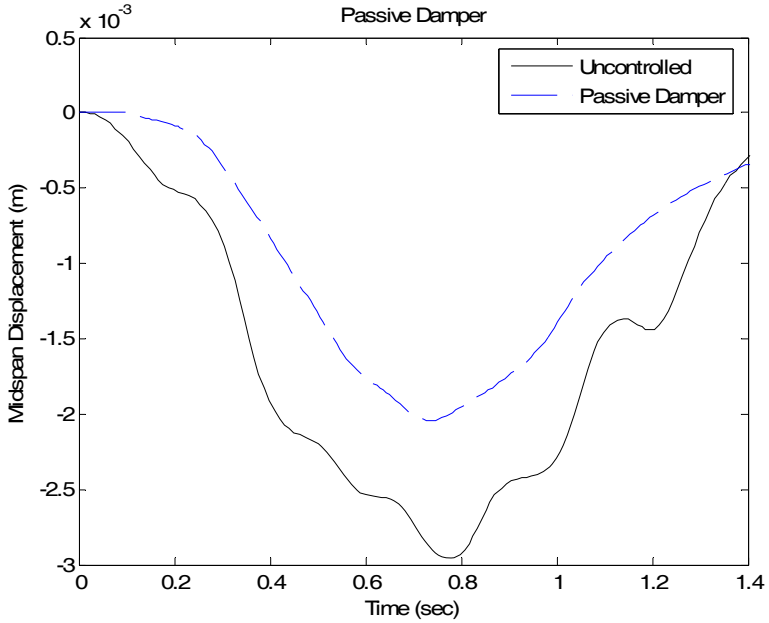

Figure 12: Passive Damper Performance

The individual performances of the control devices with optimal device parameters are illustrated in Figures 9 through 12. As intended in design, the active control device reduces peak midspan displacement by approximately 50%, specifically 50.13%. The semiactive control device displays comparable performance capable of reducing peak midspan displacement by 49.79%. While the passive stiffener reduces peak midspan displacement by 47.72% and the passive damper reduces peak midspan displacement by 30.78%.

2.7 Robust Performance of Structural Control Strategies

The performance of each control strategy is evaluated by investigating various loading scenarios and structural parameters. The various loading cases entail a range of truck speeds and the various structural parameters include a range of bridge stiffness values, analogous to a change in bridge length.

The device parameters for the passive damper and stiffener, c_d and k_d, are physical quantities which can be changed only by physically altering the device. Thus the device parameters, c_d and k_d, for these two control strategies are selected only once for the original Cromwell Bridge, and employed for each of the various structural parameter scenarios.

Alternatively, for the active and semiactive devices the device parameters of the control strategies are not physical values; they are numerical, housed within the control algorithm of the device. This characteristic allows the optimal parameters, $Q_{lqr,}$ and K_{lqr}, to be selected specifically for the individual structural application. For this study a range of bridge lengths is investigated, for every bridge length evaluated specific optimal device parameters are determined.

Simulations were conducted to demonstrate what class and type of control strategy is most prominently and efficiently able to mitigate heavy traffic induced bridge vibrations. The criterion for evaluation is performance efficiency and robustness of the control device. The measure of evaluation is the percent reduction the control device affords in peak midspan displacement subjected to a single truck loading.

The performance of each control strategy is evaluated by investigating varying loading scenarios and structural parameters. The varying loading cases encompass a range of truck speeds. The speed of the truck range from 8.94m/s (29.33ft/s, 20mph) to 35.76m/s (117.33ft/s, 80 mph); the speed limit across the Cromwell Bridge is 29.06m/s (95.33ft/s, 65 mph). The varying structural parameters include a range of bridge stiffness values, analogous to a change in bridge length. The bridge length range selected is half of the length of the Cromwell Bridge to twice the length of the Cromwell Bridge.

The robustness of each control strategy is evaluated by considering the device performance over the range of truck speeds and bridge lengths. In this study a device which demonstrates generally invariant performance behavior over a range of loading cases or bridge parameter scenarios is considered robust.

The simulations were run using 40 shape functions; which included one static deflection and 39 mode shapes. For every simulation, the control device attachments were located at $\alpha = 0.2$ and a scissor magnification factor of 5.0 was used.

The simulations were conducted using Matlab and Simulink. A variable-step ODE 45 solver with a relative tolerance of 1e-3 was used for all cases excluding the semiactive control device which used a fixed-step ODE 3 solver with a step size of 1e-5. The performance results from the numerical testing are graphically summarized in Figures 13 and 14.

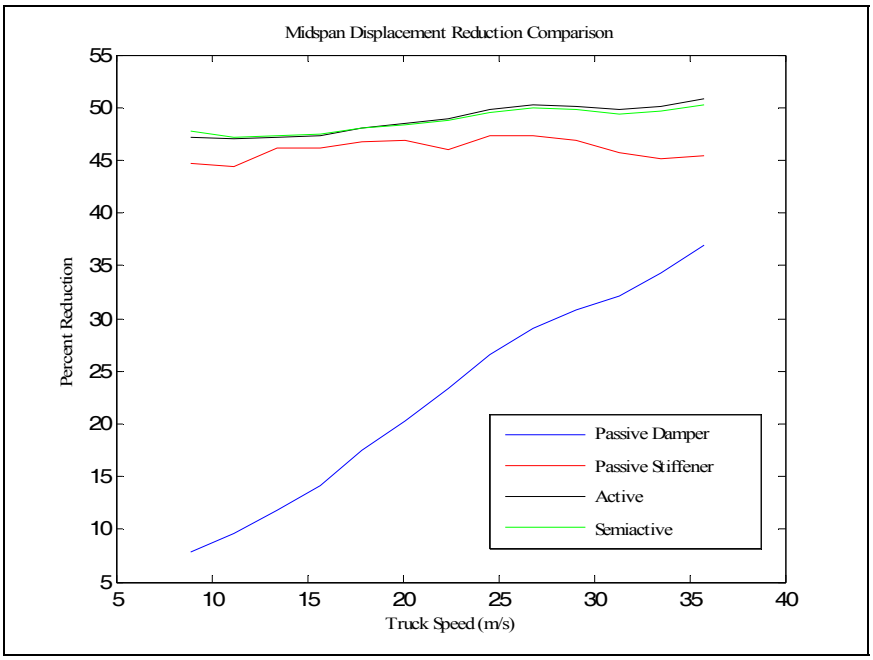

Figure 13: Control device performance summarized over a range of truck load speeds

Figure 13 illustrates the performance of each control device subject to various loading conditions. The results in their entirety assess the robustness of each control device for the range of loading conditions. These results show that the active and semiactive control devices demonstrate performance behavior that is nearly identical and achieve performance efficiency greater than the passive devices. The passive stiffener performance is very close to that of the active and semiactive control devices. And in all cases the performance efficiency of the passive damper falls well below the performance efficiency realized by any of the other control devices.

The passive stiffener, active, and semiactive control devices each demonstrate robustness. The performance behavior is consistent over the range of vehicle speeds; considering all three of these devices the performance efficiency ranges only from around 44% -51% reduction of midspan displacement for all truck speeds investigated.

The efficiency of the performance and robustness is further demonstrated by recalling that the passive stiffener, active device, and semiactive device were all designed to produce a midspan displacement reduction of approximately 47% - 50%.

Figure 14 summarizes the results obtained for various bridge parameters while employing identical physical control devices to each bridge configuration. The results illustrate the performance of each of the four control devices subject to each structural parameter variation. The results in their entirety assess the robustness of each control device for the range of bridge properties.

A stiffness factor of 8 corresponds to a bridge 8 times as stiff as the Cromwell Bridge; a bridge of half the length of the Cromwell Bridge. A stiffness factor of 0.125 corresponds to a bridge 0.125 times as stiff and the Cromwell Bridge; twice the length of the Cromwell Bridge.

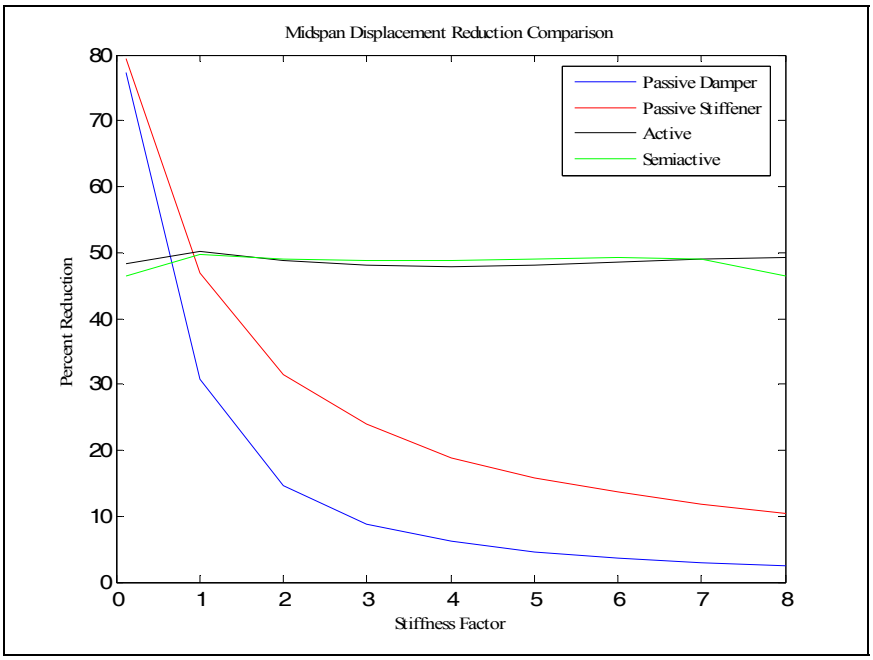

Figure 14: Control device performance summarized over a range bridge lengths

For the vast majority of the stiffness range the active and semiactive control devices perform superiorly compared to the passive devices. Additionally, these two devices perform very near the targeted reduction value of approximately 50 % for the entire stiffness range. For the stiffness value of 0.125, the passive devices achieve better performance efficiency than the active and semiactive devices. This can be attributed to the fact that the device force developed is much greater in the passive devices (around 244.65 kN (55 kips) for each device). This is because, for the passive devices, the physical control parameters are not individually designed for each structural parameter scenario investigated. Conversely, for the semiactive and active devices the device force is limited (124.55 kN (28 kips)) for each structural parameter scenario and these device parameters are redesigned for each structural parameter scenario investigation. Ideally the active and semiactive devices could achieve performance as great as the passive devices demonstrate if the control design constituents were changed.

For the active and semiactive devices the results exhibit robust behavior. These results allude to the idea that control devices of the active and semiactive nature can efficiently and effectively offer midspan displacement reductions to a multitude of bridges without being redesigned for every individual bridge. Where as to achieve a 50% displacement reduction using either the damper or stiffener, the device would have to be designed and built specific to the bridge of interest.

2.8 Conclusions on Structural Control to Reduce Traffic Induced Bridge Vibration

The purpose of this study was to examine mitigating heavy vehicle traffic induced highway bridge vibrations utilizing several structural control strategies. This investigation was conducted by developing an analytical model for an in service highway bridge under heavy vehicle truck loading. Three primary classes of structural control devices were considered for the study. Four types of devices were designed to be investigated through analytical testing; passive stiffener, passive damper, active device, and semiactive device. The bridge system with integrated control

device was tested for various loading cases and structural parameter values in order to observe the performance efficiency and robustness that each device was able to achieve.

The results obtained from the simulations illustrate the effectiveness of each of the devices over a range of loading cases and bridge parameters. Results summarize the performance efficiency and robustness of the active and semiactive devices were far greater than either of the passive devices.

Considering results from the simulations as well as characteristics of the control strategies, the semiactive device is selected as the forefront device for this particular application. The semiactive controller offers several benefits over the other devices while still affording performance levels and robust behavior very near that of the active control device, which achieves the highest performance efficiency. The benefits of the semiactive device over its competitors include: it requires little energy to operate, it is controllable in real time, and it is inherently stable. Additionally, the semiactive device exhibits a multi-bridge application characteristic. More specifically, one semiactive device can be designed and that design can be used on many different bridges, while still offering consistent performance and behavior. This is demonstrated through the robustness of the semiactive device displayed in the numerical testing results.

This paper considers the feasibility and benefits of using a structural control strategy to mitigate vehicle induced vibration of a highway bridge. The findings support the selection of a semiactive control device for reducing heavy vehicle traffic induced bridge vibrations.

3. Development of a Coherence-Based Structural Health Monitoring Method for Semiactive Controlled Structures

This study develops and evaluates a SHM method for identifying local nonlinear damage on a highway bridge. A typical in service highway bridge is selected for the study and a numerical model of the highway bridge with truck loading is developed. A semiactive control strategy is described and the device is employed to excite the highway bridge with a random white noise command for monitoring purposes. The proposed SHM method utilizes the coherence relationship between the semiactive device input and the midspan acceleration vibration response output. An analytical study is conducted to investigate the capability of the SHM method to accurately and precisely detect local nonlinear damage. Results from the study demonstrate a high sensitivity of the SHM method to identify local nonlinear damage. The proposed SHM method is unique in several respects: a semiactive structural control device is used to excite the structure (rather than traditional application of vibration mitigation) and the coherence function is utilized as a tool to detect local nonlinear damage.

3.1 Literature Review of Structural Health Monitoring

There exists a responsibility to insure the safety of the structures established for and used by the public. Structural health monitoring (SHM) is the practice of identifying the presence, location, and severity of structural damage. SHM fosters a procedure for ensuring safe structures and preventing deterioration through timely maintenance. A clear need for SHM is comprehensible when evaluating the condition of the nation's infrastructure. For example, there are nearly 600,000 public highway bridges in the United States (Kirk and Mallet, 2007), about 90% of all personal travel and 80% of all freight travel is accommodated on highways traveling over these

bridges (Friedland and Small, 2003). In 2006 over 74,000 (12%) of the total bridges in the nation were categorized as structurally deficient; meaning there is an eminent need of repair, rehabilitation, or reconstruction (Kirk and Mallet, 2007, Friedland and Small, 2003) of the structure.

Structural health monitoring includes methods of visual inspection, non-destructive evaluation (NDE), and vibration based identification. Visual inspection is a common method of health monitoring. Visual inspection, however, is neither objective nor reliable, containing great uncertainty in identifying the existence, location and degree of damage (Doebling et. al, 1996, 1997, 1998).

New technologies for the NDE of civil structures include ultrasonic testing, penetrant testing, visual testing (different than visual inspection), magnetic particle testing, radiographic testing, acoustic emission, eddy current testing, and thermal field methods (U.S. DOT, 2001, Chang, 1997, Chase and Washer, 1997). These technologies determine local damage and typically require the general region of damage on the structure to be first identified. For many structures, locating the damage prior to inspection is difficult. Further, most of these methods require that the portion of the structure being inspected is readily accessible.

Vibration measurements are a less subjective method for SHM. Vibration based SHM fosters global as well as local evaluation of the structure. As such, vibration based techniques are receiving much recent attention (Farrar et. al, 1994, Chakrabarty and Okaya, 1995, Salawu and Williams, 1995, Farrar and Doebling, 1997, Salawu, 1997, Doebling et al., 1998, Farrar et. al, 2000, Caicedo et. al, 2000, Chang, 2000). Vibration based damage detection is considered rather intuitive; as it presumes that damage alters the stiffness, mass, or damping properties of the system, which results in a change in the dynamic response of the system (Farrar et al., 2000). Damage is typically identified through interpretation of changes in the systems vibration characteristics (i.e. natural frequencies, damping ratios, modes shapes). Vibration based methods require monitoring at predefined locations on the structure, where the monitored locations do not need to be at the location of the damage.

There are, however, a number of challenges associated with vibration based SHM. Vibration based identification relies on employing ambient vibration or operational loads, which can often prove difficult. These excitations often tend to excite the lower frequency global modes that can be insensitive to local damage (Sohn, 2001). Sensitivity to local damage and small flaws is critical to permit health monitoring to identify damage in time for repair. Additionally, environmental and operational variability of civil structures can affect the natural frequencies and mode shapes, rendering SHM methods that rely on changes in these parameters ineffective except in the presence of extreme damage (Sohn, et. al, 1999, Olund, 2006). Another challenge is the inability of most vibration based SHM methods to detect nonlinear behavior, such as the opening and closing of fatigue cracks in structural members or connections. Despite the challenges associated with vibration based identification methods for SHM these methods continue to receive much attention.

Structural control devices are primarily designed to mitigate the vibrations of structures and accordingly the damage to structures, with a goal of extending the life of structures. Although structural control devices have shown promise in application, the possibility of damage resulting from extreme events and long-term service life of a structure is certainly possible. Of recent interest is the concept of using a structural control device on a structure to simultaneously mitigate vibration, increase safe life, and monitor health.

A recent project in California has investigated the combination of structural control and structural health monitoring for highway bridges (Johnson, 2003, Elmasry and Johnson, 2004). Variable stiffness and damping devices (VSDDs) are considered for the study. This analytical research demonstrates that more accurate estimates of structural characteristics can be achieved through the use of controllable stiffness and damping technology by allowing parametric changes to the structure's stiffness and damping characteristics. Parametric changes to the structure's stiffness and damping characteristics allow for multiple structural responses to be accomplished under a single force type, thus fostering a very effective method for system identification.

A similar approach is taken for a system integrating structural control and structural health monitoring for buildings (Xu and Chang, 2007). The research explores employing semiactive friction dampers to mitigate earthquake induced vibrations of a building while simultaneously utilizing the semiactive devices to develop and establish a SHM procedure. The SHM procedure identifies structural parameters by adding known stiffness values to the system via the semiactive friction dampers. The identification of the structural parameters is based on model updating by looking at two states of the building: the original building and the building with added stiffness; and thus providing a reference state for subsequent damage.

The research presented in this work investigates employing a semiactive structural control device on a highway bridge to perform SHM. More specifically, this paper proposes a SHM procedure capable of identifying local nonlinear damage on a highway bridge. A typical in service highway bridge is selected for the study and a numerical model of the highway bridge with truck loading is developed. The semiactive structural control strategy is then introduced and the proposed SHM procedure and application are discussed. A closing crack is selected as damage to the structure; the nonlinear effects associated with closing cracks are introduced into the model to investigate the capabilities of the proposed method to accurately and precisely detect the local nonlinear damage. Finally, simulation results illustrating the efficiency and effectiveness of the proposed SHM technique are presented.

3.2 Proposed Coherence Based Structural Health Monitoring Method

In this study, the system of interest is the Cromwell Bridge; by the previously described configuration the system is of a multiple input single output nature. The two inputs for the system are the truck loading and the device force. The single output for the system is selected as the midspan acceleration vibration response of the bridge.

Multiple input single output systems are frequently described by the multiple coherence function, $\gamma_{y:x}(f)$, a correlation relationship between the system's output and the system's multiple inputs. For a constant parameter linear system the multiple coherence function is equal to unity.

For uncorrelated inputs there is a linear relationship between the multiple coherence function and ordinary coherence of the individual input to output relationships, Equation (14) demonstrates this relationship for a two input single output system.

$$\gamma_{y:x}^2(f) = \gamma_{1y}^2(f) + \gamma_{2y}^2(f) = 1.0 \tag{14}$$

where $\gamma_{1y}(f)$ is the coherence between input 1 and the output and $\gamma_{2y}(f)$ is the coherence between input 2 and the output. Uncorrelated inputs greatly simplify calculating the multiple coherence function (Bendat and Peirsol, 2000).

For mitigating traffic induced bridge vibrations the truck loading is used to generate the control algorithm for the semiactive device and therefore from Equation (3) the inputs are correlated. Alternatively, for monitoring purposes, the truck loading is used to power the semiactive device which in turn generates an uncorrelated random vibration input. This is possible because of the use of the smart structure; the device can be controlled in real time and utilized to produce any desired dissipative force. So for monitoring purposes, the semiactive device is used to randomly excite the structure rather than provide forces for vibration mitigation. For SHM purposes the semiactive device produces a random band limited white noise excitation which is applied to excite the bridge. The random input achieved by the semiactive devices for SHM purposes ensures that the inputs in this investigation are indeed uncorrelated. This simplifies the multiple coherence relationship, making it linear and thus allowing the input output relations to be viewed individually (essentially 2 SI/SO systems) as shown by Equation (14).

For a SI/SO system the relationship between the input and the output is often described by the ordinary coherence function, $\gamma_{yx}(f)$. The ordinary coherence function is a real valued measure that quantifies the correlation of the system's input to the system's output. For a linear system, the ordinary coherence function can be interpreted as the fractional portion of the mean square value of the output that is contributed by the input at frequency *f* (Bendat and Piersol, 2000). Constant parameter SI/SO linear systems exhibit a coherence of unity.

Of interest is when the coherence function for a constant parameter linear system with a SI/SO exhibits behavior other than unity. For situations where the coherence function is between unity and zero, there are 3 possible physical situations that can exist: extraneous noise is present in the measurements, the system relating the input and output is not linear and/or the output is due to multiple inputs.

The one-sided auto and cross spectral density functions of a system can be utilized to express the ordinary coherence function of a SI/SO system

$$\gamma_{xy}^2(f) = \frac{\left|G_{xy}(f)\right|^2}{G_{xx}(f)G_{yy}(f)} \tag{15}$$

where $G_{xy}(f)$ is the one-sided cross spectra and $G_{xx}(f)$ and $G_{yy}(f)$ are the one-sided auto spectra of the input and output respectively. For this work the spectral density functions are defined using finite Fourier transforms

$$G_{xy}(f) = 2\lim_{T\to\infty}\frac{1}{T}E\left[X^*(f,T)Y(f,T)\right] \tag{16}$$

$$G_{xx}(f) = 2\lim_{T\to\infty}\frac{1}{T}E\left[\left|X(f,T)\right|^2\right] \tag{17}$$

$$G_{yy}(f) = 2\lim_{T\to\infty}\frac{1}{T}E\left[\left|Y(f,T)\right|^2\right] \tag{18}$$

where $X(f,T)$ and $Y(f,T)$ represent the finite Fourier transforms of the input and output respectively. For this investigation, it is assumed that the input, semiactive device force (*y*), and output, midspan acceleration vibration response (*x*), are stationary over the record length.

Midspan displacement, midspan strain, and damper force time histories for the system with no control, semiactive control, and random excitation can be seen in Figures 5 through 7. The time history plots shown in Figures 5 through 7 are for a 331.4 kN (70 kip) truck traveling at a speed of 29.1 m/s (65 mph).

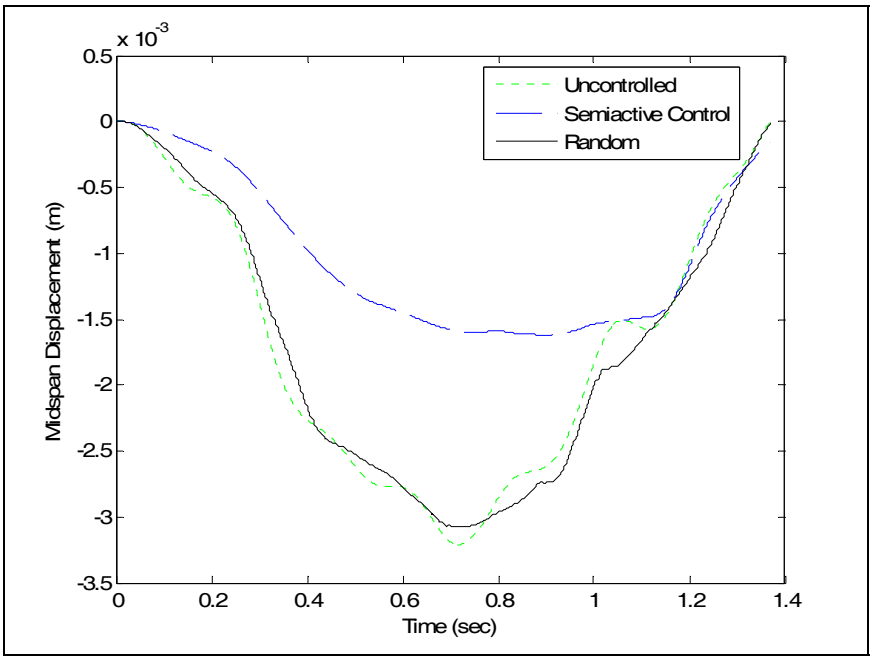

Figure 15: Displacement Time History without Damage

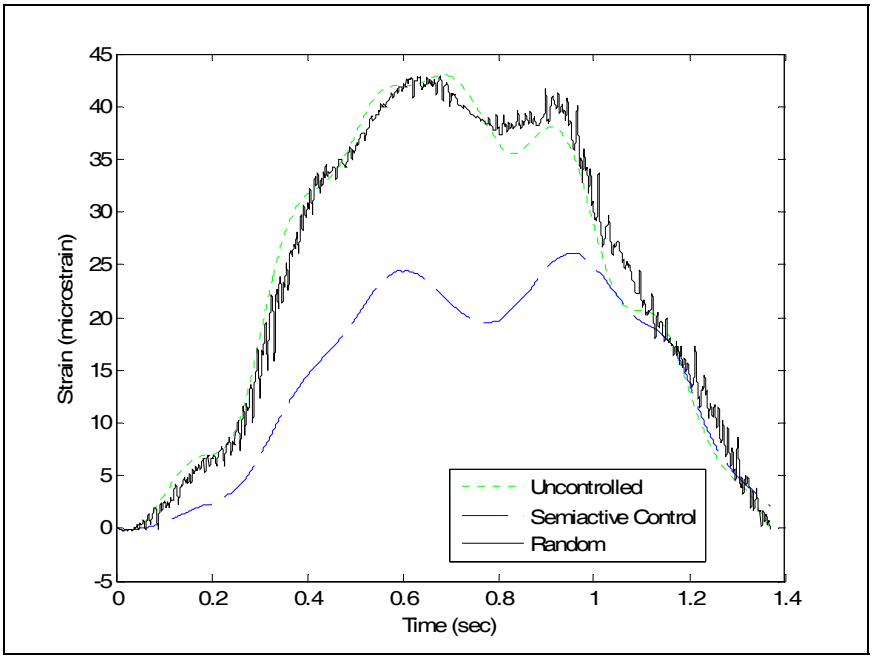

Figure 16: Strain Time History without Damage

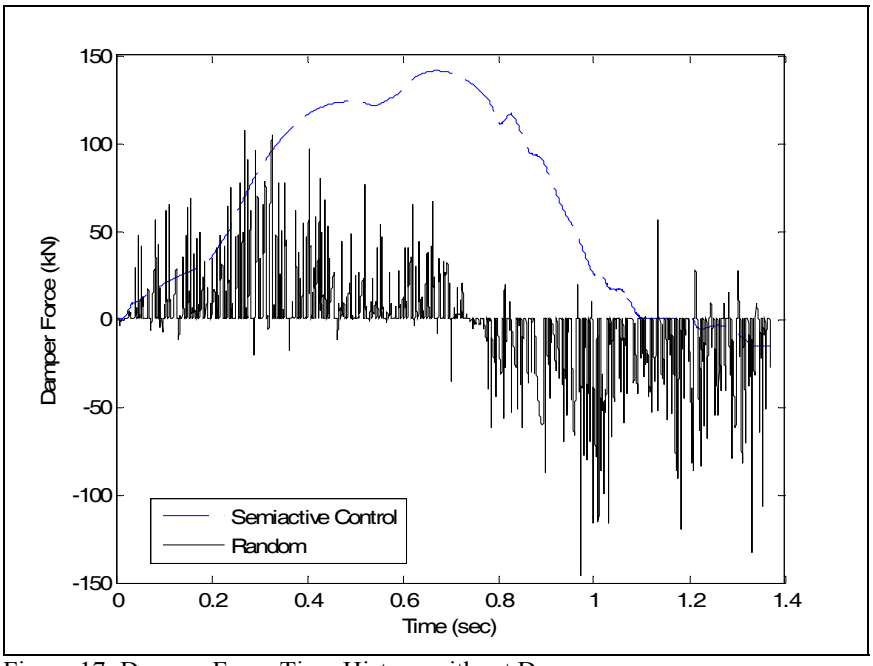

Figure 17: Damper Force Time History without Damage

3.2.1 Results for the Undamaged Structure

The ordinary coherence relationship is proposed for use to monitor the structure; specifically, the ordinary coherence between the semiactive device input and midspan acceleration vibration response output. This ordinary coherence relation is utilized to develop the proposed SHM procedure.

A sequence of 70 random trucks cross the highway bridge (ADTT of the bridge is approximately 8,145); the mean truck weight is 289.1 kN (65 kips) with a standard deviation 44.5 kN (10 kips) and the mean truck speed is 29.1 m/s (65 mph) with a standard deviation of 4.5 m/s (10 mph). The motion of the bridge due to the truck passages enables the semiactive control device to be implemented into the system. For SHM purposes the semiactive device is commanded to produce dissipative forces of a random nature, thus ensuring the two inputs of the system are indeed uncorrelated. These random forces are characterized as a white noise signal with a specified bandwidth. The white noise has an expected peak device force of 133.4 kN (30 kips) with a standard deviation of 66.7 kN (15 kips) and a mean value of 0 kN (0 kips). The white noise is filtered by a bandwidth specified as 200 Hz and applied using a 12^{th} order low pass Butterworth filter.

During this process of truck passage and semiactive device random excitation the device force and acceleration vibration response at midspan are measured. Sensor noise is included in the evaluation and modeled in the system as band limited white noise. The sensor noise is added to the collected signals, semiactive device force and midspan acceleration vibration response. The noise signals have an expected mean value of 0.1% the peak expected peak values of the measured signals with RMS values $1/3^{rd}$ of the peak noise signal values.

The one-sided auto spectral density functions for the collected signals of interest, semiactive device force and midspan acceleration vibration response, are presented in Figures 8 and 9. Figure 8 shows that the energy of the semiactive device force is indeed generally constant over the excitation range, as intended by employing the white noise excitation. Figure 9 shows that the majority of the energy of the acceleration vibration response is concentrated at the first bending mode natural frequency of the structure.

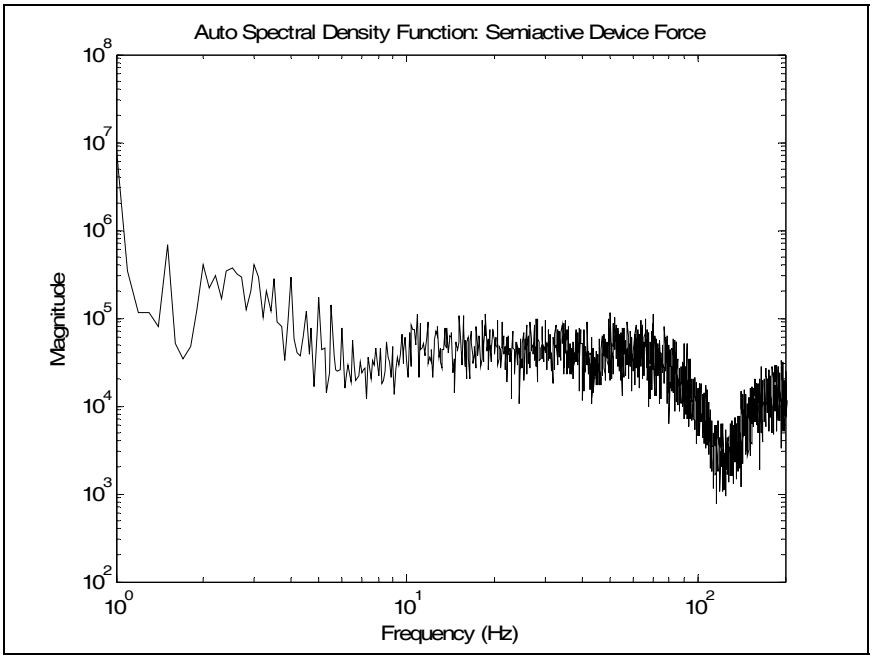

Figure 18: Auto Spectral Density Function: Semiactive Device Force

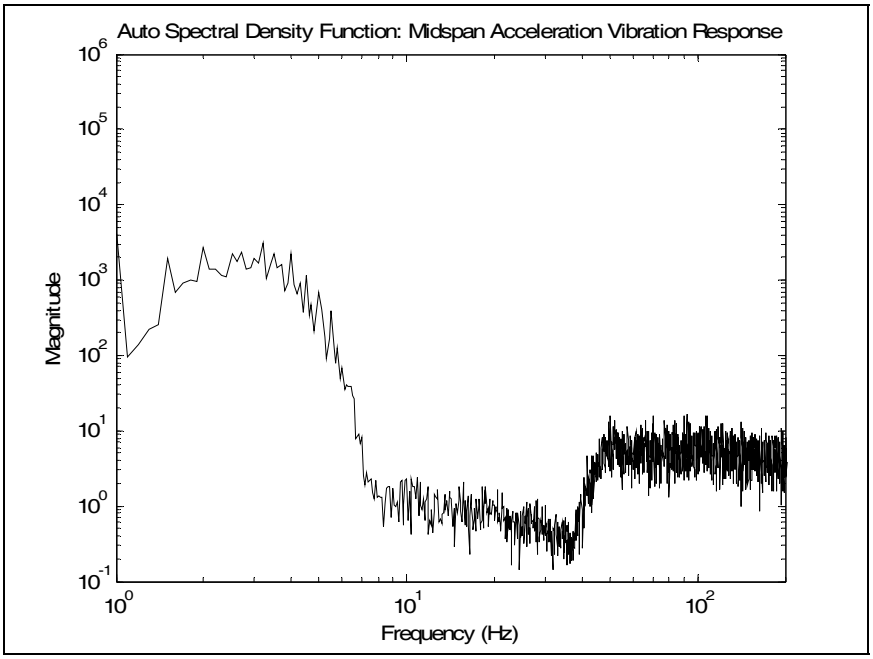

Figure 19: Auto Spectral Density Function: Midspan Acceleration Vibration Response

An ordinary coherence relation is developed using the collected signals. Figure 20 illustrates the ordinary coherence relationship between the semiactive device input and midspan acceleration vibration response output, including signal sensor noise. The time step for the simulations used to generate Figure 20 was 1e-4 sec correlating to a sampling frequency of 10 kHz. The number of fast Fourier transforms selected for the processing was 1e4, resulting in a frequency step size of 1 Hz and 140 averages.

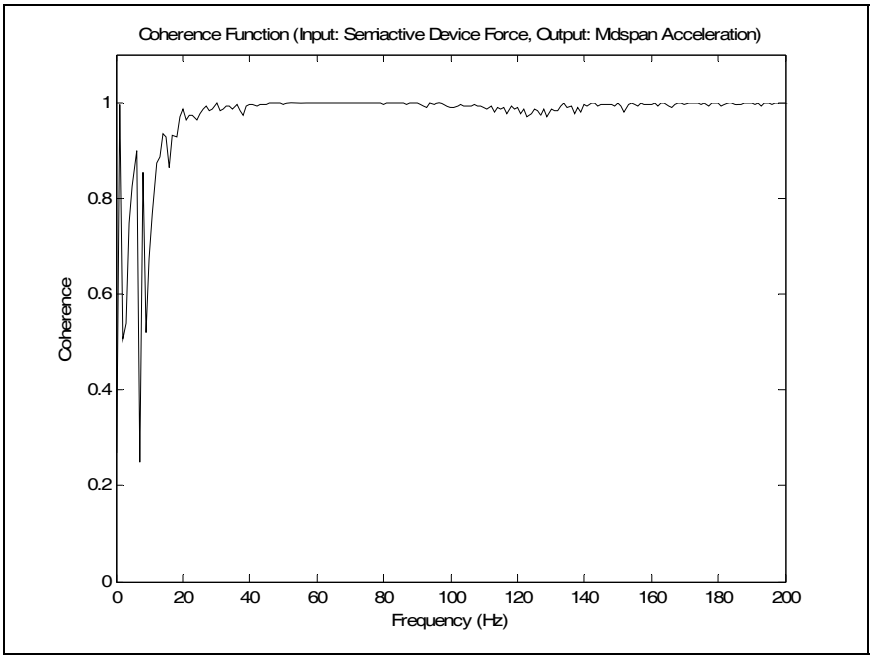

Figure 20: Coherence Function: Damper Force Input and Midspan Acceleration Vibration Response Output

The coherence relationship developed between the semiactive device input and midspan acceleration vibration response output is employed to monitor the system. As previously stated, when the coherence strays from unity there is an indication of three possible physical situations: extraneous noise present in the measurements, nonlinear behavior, and/or multiple input responses. These phenomena are utilized for SHM as a format to classify the system and detect damage.

In order to utilize the specified coherence relationship for SHM, the system behavior should be understood and generalized. The following gives a description of the coherence relation of interest for the system being investigated, shown in Figure 20. For the system the sensor noise associated with collecting the data is modeled in the system, as such it is assumed no additional or extraneous noise exists. The coherence of the system is not at unity below 20 Hz. This behavior can be attributed to a nonlinear system or multiple inputs. The system was developed as a linear model, and therefore the coherence behavior below 20 Hz is ascribed to the presence of multiple inputs. In the range of 0 Hz to 20 Hz the system response is due to the two inputs; the truck force and the semiactive device force excite the bridge in this frequency range. Above 20 Hz the coherence is essentially unity. Meaning the system is acting as a single SI/SO system in this range. Only the semiactive device is exciting the bridge in this frequency range, the semiactive device linearly controls the bridge response in this higher frequency range.

3.3 Simulating Local Bridge Damage

For this study, damage is selected as a crack located in a longitudinal component of the substructure of the bridge, essentially a girder or cover plate. More specifically, a closing crack is assumed for the damage. The vibratory behavior of cracked beams has been investigated thoroughly by a large number of researchers; see Dimarogonas (1996) for an extensive overview.

A closing crack, often termed a breathing crack, opens and closes during the cyclic deformation of a structure. The vibratory behavior and modeling techniques of this category of cracks has been studied thoroughly by researchers (Bovsunovsky and Bovsunovsky, 2007, Bovsunovsky and Surace, 2005, Saavedra and Cuitino, 2001, Pugno et al., 2000, Dimarogonas, 1996, Ruotolo et al., 1996). The mathematical modeling of such cracks is typically based on the assumption that the crack periodically closes and opens, where the opening and closing of the crack leads to instantaneous changes in the structure's stiffness.

The dynamic behavior of a vibrating system is significantly nonlinear in the presence of a closing crack (Bovsunovsky and Bovsunovsky, 2007). Effects associated with the nonlinearity of the system are characteristic of a vibrating system with a closing crack. These nonlinear effects include: the appearance of subharmonic and superharmonic resonances and significant nonlinear behavior of the vibration response (displacement, acceleration, strain, etc.) at the subharmonic and superharmonic resonances (Bovsunovsky and Surace, 2005). Extensive research investigating the presence of the subharmonics and superharmonics has been preformed; showing subharmonic and superharmonic resonances occurring at integer multiples of the forcing frequency (Saavedra and Cuitino, 2001, Ruotolo et al., 1996) and at integer multiples of the structure's natural frequencies (Bovsunovsky and Bovsunovsky, 2007).

The nonlinear effects exhibited by a cracked beam are much more sensitive to the presence of cracks than the changes in natural frequencies or mode shapes (Bovsunovsky and Surace, 2005). This characteristic enables the revealing of nonlinear behavior to be a very sensitive method for crack detection. Much research has been dedicated to correlating the level and response of nonlinearity to the quantitative evaluation of damage parameters (type, size, location) (Bovsunovsky and Surace, 2005, Ruotolo et al., 1996).

Of interest in this particular study was to determine the potential of the developed SHM technique at detecting local nonlinear damage, specifically closing cracks. To evaluate the proposed method the effects of the crack are modeled. Effectively the nonlinear effects characteristic of a closing crack are modeled rather than the physical crack. The effects are modeled as a harmonic frequency; representing a subharmonic or superharmonic resonance. The capability of the developed SHM procedure is demonstrated by the ability of the method to detect the nonlinear behavior at subharmonic and superharmonic resonances.

The nonlinear harmonic frequency representing the behavior of a closing crack is modeled as an additional output to the system. This additional output signal representing the nonlinear behavior of the opening and closing of the crack is selected as sinusoidal and added to the vibration response of interest. The sinusoidal signal has an amplitude of approximately 1% of peak vibration response being measured, midspan acceleration, and is selected to have an arbitrary frequency of 90 Hz. Note that any frequency within the excitation capabilities of the semiactive control device could potentially be selected.

3.4 Structural Health Monitoring Procedure and Results

The dynamic behavior of the system is characterized by the coherence function between the semiactive device input and midspan acceleration vibration response output. This coherence function relation is established as the reference state for the SHM procedure.

Damage is introduced to the system as an additional sinusoidal input having an amplitude of approximately 1% of peak vibration response and a frequency of 90 Hz. The dynamic behavior of the system is again characterized by the coherence function between the semiactive device input and midspan acceleration vibration response output. This coherence function is established as the damaged state.

The reference state and damage state are determined identically. A series of 70 random trucks cross the highway bridge; the mean truck weight is 289.1 kN (65 kips) with a standard deviation 44.5 kN (10 kips) and the mean truck speed is 29.1 m/s (65 mph) with a standard deviation of 4.5 m/s (10 mph). The ADTT of the Cromwell Bridge is approximately 8,145 trucks; meaning the coherence relation can be determined in approximately 15 minutes. The semiactive device is commanded to produce dissipative forces of a random nature; these random forces are characterized as a white noise signal with a specified bandwidth. The white noise has an expected peak device force of 133.4 kN (30 kips) with a standard deviation of 66.7 kN (15 kips) and a mean value of 0 kN (0 kips). The white noise is filtered by a bandwidth specified as 200 Hz and applied using a 12^{th} order low pass Butterworth filter. Sensor noise is modeled in the system as band limited white noise and added to the collected signals. The noise signals have an expected mean value of 0.1% the expected peak values of the measured signals with RMS values $1/3^{rd}$ of the peak noise signal values. Using the measured quantities from the semiactive device force and midspan acceleration vibration response the reference state and damage state coherence relations are developed. The time step for the simulations was 1e-4 sec and the sampling frequency was 10 kHz. The number of fast Fourier transforms selected for the processing was 1e4, resulting in a frequency step size of 1 Hz and 140 averages.

The reference state and damage state are compared to evaluate the sensitivity and effectiveness of the SHM method. Damage is classified as a change in the system. The goal of the described SHM method is to identify accurately and precisely local nonlinear damage. Figure 11 shows the simulation results for the reference state and damage state.

Figure 11 illustrates the ability of the SHM procedure to accurately and precisely identify the damage to the system. The nonlinear behavior characteristic of the damage is clearly picked up through the capacity of the SHM procedure, shown as a dominant antipeak in Figure 21. Intrinsic of the coherence function is the departure from unity in the presence of nonlinearity in the system. The SHM is highly proficient at detecting accurately and precisely the nonlinear behavior characteristic of the local damage.

The one-sided auto spectral density function for the midspan acceleration vibration response is presented in Figure 22. The spectral density function is capable of detecting the damage to the system, observed as a peak at 90 Hz. However, if the discrete frequencies of the fast Fourier transform do not coincide with the damage frequency, the damage may not be observable. Rather the damage would be distributed to the discrete frequencies neighboring the damage frequency, due to the property of spectral leakage, making the damage less observable (Bendat and Piersol, 2000).

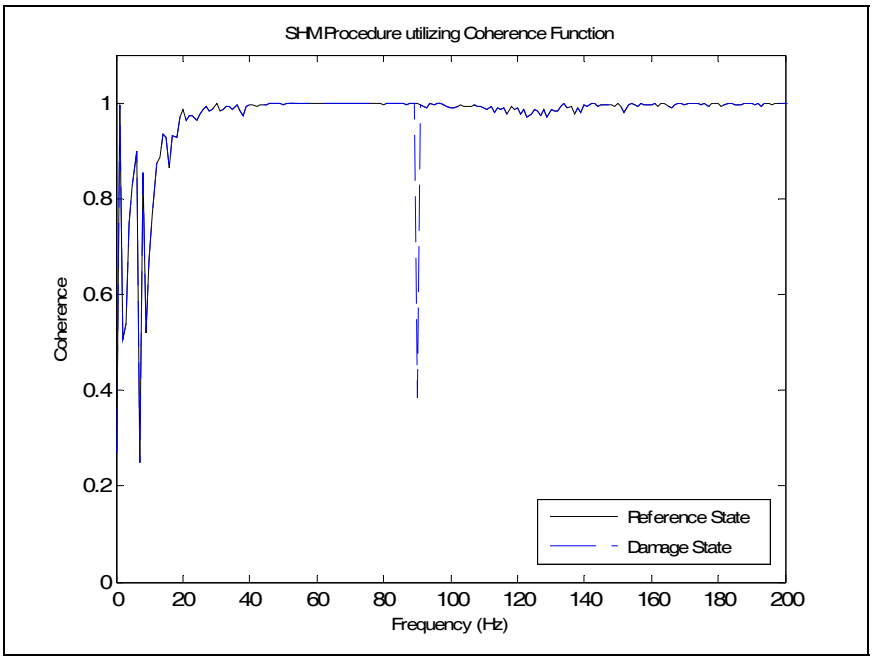

Figure 21: SHM Procedure: Comparing Reference State and Damage State utilizing Coherence Relation between Semiactive Device Input and Midspan Acceleration Vibration Response Output

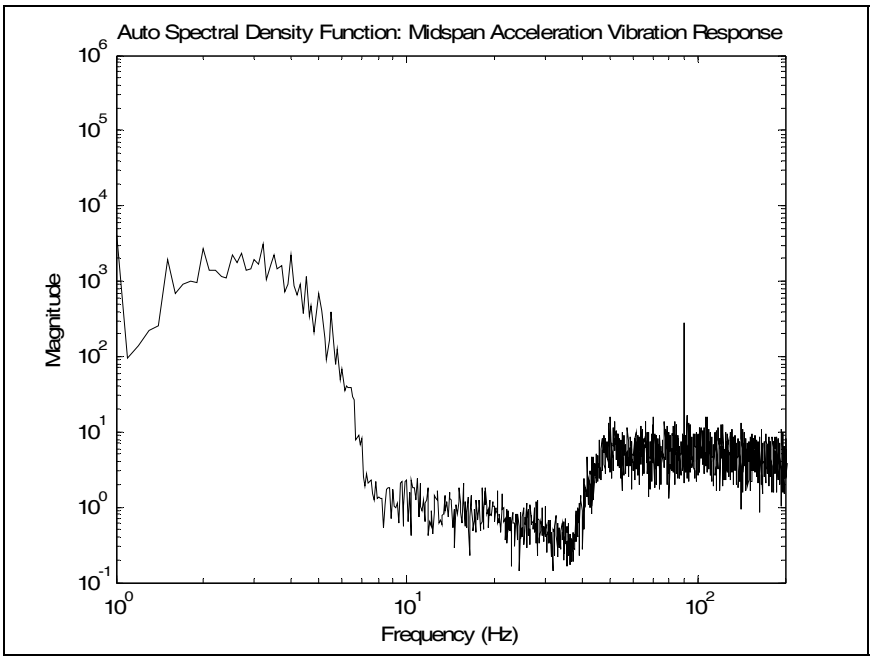

Figure 22: Auto Spectral Density Function: Midspan Acceleration Vibration Response Output with Damage

3.5 Conclusions on SHM using Semiactive Control Devices

The purpose of this study was to develop and evaluate a SHM method for identifying local nonlinear damage of a highway bridge. An analytical model for an in service highway bridge under heavy vehicle truck loading is developed and used for the study. A semiactive control device strategy is described; the device is used to excite the highway bridge with a random white noise command. Damage is selected as a closing crack and introduced to the highway bridge

model. The effects of the closing crack are modeled, selected as a sinusoidal signal of arbitrary frequency and amplitude of 1% of the peak vibration response signal being measured. A SHM procedure employing the coherence function is proposed. The proposed SHM method is evaluated by investigating the method's ability to accurately and precisely detect local nonlinear damage. Results of the analytical study demonstrate a high sensitivity of the SHM method to identify local nonlinear damage accurately and precisely.

The proposed SHM method is unique in several respects. First, semiactive control devices are traditionally used for structural vibration control, in the proposed SHM method the semiactive control device is employed to excite the structure with vibrations over a large frequency range. Second, the proposed SHM method utilizes the coherence relationship to detect nonlinear damage, capitalizing on an intrinsic characteristic of the coherence function.

The proposed SHM method is certainly feasible for application. Utilizing structural control devices to create safer and more cost effective structures has been explored and endorsed by many researchers. Making use of structural control devices for dual purposes, vibration mitigation and health monitoring, could potentially foster safer, more reliable, and more cost effective structures and monitoring programs; significantly benefiting the public in all aspects.

4. References

AASHTO LRFD Bridge Design Specifications, 3rd Edition (2004). American Association of State Highway and Transportation Officials, 2004.

Beer F.P., Johnston E.R., and DeWolf J.T. (2006). Mechanics of Materials, 4th Edition. MCGraw Hill Inc., New York.

Bendat, J.S. and Piersol, A.G. (2000). Random Data Analysis and Measurement Procedures, Wiley Series in Probability and Statistics, John Wiley and Sons, New York.

Bovsunovsky A. and Bovsunovsky O. (2007) "Crack Detection in Beams by Means of the Driving Force Parameters Variation at Non-Linear Resonance Vibrations." *Key Engineering Materials,* Vol. 347 pp. 413-20.

Bovsunovsky A.P. and Surace C. (2005) "Considerations regarding Superharmonic Vibrations of a Cracked Beam and the Variation in Damping Caused by the Presence of a Crack." *Journal of Sound and Vibration,* Vol. 288, pp. 865-86.

Caicedo, J., S.J. Dyke and E.A. Johnson (2000) "Health Monitoring Based on Component Transfer Functions," *Advances in Structural Dynamics,* (Ko, J.M. and Y.L. Xu, eds.) Vol. II, pp. 997-1004.

Cardini, A.J. (2007). "Structural Health Monitoring and Development of a Bridge Weigh-In-Motion System for a Multi-Girder Steel Composite Bridge," Masters Dissertation, School of Civil and Environmental Engineering, University of Connecticut, Storrs, CT, 2007.

Chakraborty, A. and D. Okaya (1995) "Frequency-time Decomposition of Seismic Data using Wavelet-based Methods," *Geophysics*, Vol. 60.6, pp. 1906-1916.

Chang, F.K. (1997). *Structural Health Monitoring: Current Status and Perspectives.* Technomic, Lancaster, PA.

Chang, F.K. (2000). *Structural Health Monitoring* 2000. Technomic, Lancaster, PA.

Chase, S.B. and G. Washer (1997). *Nondestructive Evaluation for Bridge Management in the Next Century,* Public Roads, July/August, 16-25.

Clough, R.W. and Penzien, J. (1993). Dynamics of Structures. McGraw Hill Inc., New York.

DeBrunner, V., DeBrunner, L.S., Ta, M., and Davis, J. (2001). "Embedded Computer/Communication Sub-System for Bridge Vibration Control," *IEEE Intelligent Transportation Systems Conference Proceedings,* Oakland, CA, August 25-29, 2001.

DeBrunner, V., Zhou, D., and Ta, M. (2003). "Adaptive Vibration Control of a Bridge and Heavy Truck," *IEEE Intelligent Vehicles Symposium Proceedings*, Columbus, OH, June 9-11, 2003.

DeBrunner, V., Zhou, D., and Ta, M. (2004) "On the Design of Structural Vibration Control Systems for Highway Bridges," *IEEE Intelligent Vehicles Symposium Proceedings*, Parma, Italy, June 14-17, 2004.

Dimarogonas A.D. (1996) "Vibration of Cracked Structures: A State of the Art Review." *Engineering Fracture Mechanics,* Vol. 55.5, pp. 831-57.

Doebling, S.W., C. R. Farrar, M. B. Prime, and D. W. Shevitz (1996). "Damage Identification and Health Monitoring of Structural and Mechanical Systems from Changes in their Vibration Characteristics: A Literature Review," *Report LA: I3070-MS,* Los Alamos National Laboratory, NM.

Doebling, S.W., F. M. Hemez, L. D. Peterson, and *C.* Farrar (1997). "Improved Damage Location Accuracy using Strain Energy-based Mode Selection Criteria," *AIAA-J* , Vol. 35.4 pp. 693-699.

Doebling S.W., Farrar C.R., and Prime M.B. (1998) "A Summary Review of Vibration-Based Damage Identification Methods." *The Shock and Vibration Digest*, Vol. 30.2, pp. 91-105.

Doebling, S.W., C.R. Farrar, M.B. Prime, and D.W. Shevitz (1998). "A Review of Damage Identification Methods that Examine Changes in Dynamic Properties." *Shock and Vibration Digest,* Vol. 30.

Elmasry M.I. and Johnson E.A. (2004) "Health Monitoring of Structures under Ambient Vibrations using Semiactive Devices." *Proceedings of the 2004 American Control Conference*. Boston MA.

Farrar, C. R., Baker W. B., Bell T. M., Cone K. M., Dading T. W., Duffey T. A., Ekiund A., and Migliori A. (1994). "Dynamic Characterization and Damage Detection in the I-40 Bridge over the Rio Grande." *Las Alamos Report LA- 12767-MS UC-906,* June 1994.

Farrar, C. R. and Doebling S. W. (1997). "Lessons learned from Applications of Vibration Based Damage Identification Methods to Large Bridge Structure." *Structural Health Monitoring: Current Status and Perspectives*, pp. 351-370, ed. F. K. Chang, Technomic Pub. Lancaster, PA.

Farrar C.R., Doebling S.W., and Nix D.A. (2000). "Vibration-Based Structural Damage Identification." *Philosophical Transactions of the Royal Society of London,* Vol. 359 pp. 131-49.

Friedland, I.M. and Small, E.P. (2003). "FHWA Bridge Research and Technology Deployment Initiatives," *Proceedings of the 2003 Mid-Continental Transportation Research Symposium*, Ames, IA, August 2003.

Johnson, E.A. (2003), Metrans Project Number 03-17, Innovative Bridge Structural Health Monitoring Using Variable Stiffness and Damping Devices. PI - E.A. Johnson.

Johnson, E.A. and Smyth, A. (2007), *Proceeding of the Fourth World Conference on Structural Control and Monitoring*. San Diego, July 11-13, CD-ROM edited by Johnson and Smyth.

Karoumi, R. (2000). "Modeling of Cable-Stayed Bridges for Analysis of Traffic Induced Vibrations," *Conference on Structural Dynamics Proceedings*, San Antonio, TX, February 7-10, 2000.

Kawatani, M., Kobayashi, Y., and Kawaki, H.(2000). "Influence of Elastomeric Bearings on Traffic-Induced Vibration of Highway Bridges," *Transportation Research Record*, Vol. 2.1696 pp. 76-82.

Kirk, R.S. and Mallet, W.J. (2007). CRS Report for Congress: Highway Bridges: Conditions and the Federal/State Role. Order Code RL34127.

Klasztorny, M. (2001). "Vertical Vibrations of a Multi-Span Beam Steel Bridge Induced by a Superfast Passenger Train," *Structural Engineering and Mechanics*, Vol. 12.3 pp. 267-281.

Kwasniewski, L., Wekezer, J., Roufa, G., Li, H., Ducher, J., and Malachowski, J. (2006). "Experimental Evaluation of Dynamic effects for Selected Highway Bridge," ASCE *Journal of Performance of Constructed Facilities*, Vol. August 2006 pp. 253-260.

Kwon, H.C., Kim, M.C., and Lee, I.W. (1998). "Vibration Control of Bridges under Moving Loads," *Computers and Structures*, Vol. 66.4 pp. 473-480.

Loebach, L., Christenson, R. (2008). "Examining the Effectiveness of Semiactive Structural Control to Reduce Traffic Induced Bridge Vibration."

Manual for Condition Evaluation and Load and Resistance Factor Rating (LRFR) of Highway Bridges, 1st Edition (2003). American Association of State Highway and Transportation Officials.

Museros, P. and Martinez-Rodrigo, M.D. (2007). "Vibration Control of Simply Supported Beams under Moving Loads using Fluid Viscous Dampers," *Journal of Sound and Vibration,* Vol. 300 pp.292-315.

Olund, J.K. (2006). "Long Term Structural Health Monitoring of Connecticut's Bridge Infrastructure with a Focus on a Composite Steel Tub-Girder Bridge," Masters Dissertation, School of Civil and Environmental Engineering, Univesity of Connecticut, Storrs, CT.

Patten, W.N., Kuehn, J.L., Sun, J., Song, G., and Sack, R.L. (1996). "Impact Vibration Reduction via Semiactive Vibration Absorbers (SAVA) for an Interstate Bridge," *Annual International Bridge Conference Proceedings*, Pittsburg, PA, June, 1996.

Patten, W.N., Mo, C., Kuehn, J., and Lee, J. (1998). "A Primer on Design of Semiactive Vibration Absorbers," *Journal of Engineering Mechanics*, Vol. January 1998 pp. 61-68.

Patten, W.N., Sack, R.A., and He, Q. (1996). "Controlled Semiactive Hydraulic Vibration Absorber for Bridges," *Journal of Structural Engineering*, Vol. February 1996 pp. 187-192.

Patten, W.N., Song, G., and Sun, J. (1997). "A Variable Stiffness and Damping System for Bridges," *Second Symposium on Practical Solutions for Bridge Strengthening and Rehabilitation Proceedings*, Kansas City, MO, March 24-25, 1997.

Patten, W.N., Sun, J., Li, G., Kuehn, J., and Song, G. (1999). "Field Test of an Intelligent Stiffener for Bridges at the I-35 Walnut Creek Bridge," *Earthquake Engineering and Structural Dynamics*, Vol. 28 pp. 109-126.

Patten, W.N., Sun, J., and Song, G. (1998). "Modal Testing of the I-35 Walnut Creek Bridge," *International Modal Analysis Conference & Exhibit Proceedings*, 1998.

Patten, W.N., Sun, J., and Zeng, A. (1999). "Smart Bridge Dampers (SBD)," *American Control Conference Proceedings*, San Diego, CA, June, 1999.

Pugno N., Surace C., and Ruotolo R. (2000) "Evaluation of the Non-Linear Dynamic Response to Harmonic Excitation of a Beam with several Breathing Cracks." *Journal of Sound and Vibration*, Vol. 235.5 pp. 749-762.

Reiterer, M. and Ziegler, F. (2006). "Control of Pedestrian-Induced Vibrations of Long-Span Bridges," *Structural Control and Health Monitoring*, Vol. 13 pp. 1003-1027.

Ruotolo R., Surace C., Crespo P., and Storer D. (1996) "Harmonic Analysis of the Vibrations of a Cantilevered Beam with a Closing Crack." *Computers & Structures*, Vol. 61.6 pp. 1057-1074.

Saavedra P.N. and Cuitino L.A. (2001) "Crack Detection and Vibration Behavior of Cracked Beams." *Computers & Structures,* Vol. 79 pp. 1451-1459.

Salawu, O.S. and Williams C. (1995). "Review of Full-scale Dynamic Testing of Bridge Structures." *Engineering Structures,* Vol. 17.2 pp. 113-121.

Salawu, O.S. (1997) "Detection of Structural Damage through Changes in Frequency Review." *Engineering Structures,* Vol. 19.9 pp. 718-723.

Sammartino, G., Amirouche, F., Chen, Z., and Wang, M.L. (1999). "Effects of Heavy Vehicle Speeds on the Structure and Vibration of Bridges," ASME *Innovations in Vehicle Design and Development,* Vol. 101 pp. 139-147.

Sohn, H., Farrar C.R., Fugate M.L., and Czarnecki J.J. (2001) "Structural Health Monitoring of Welded Connections," *The First International Conference on Steel & Composite Structures*, Pusan, Korea, June 14-16, 2001.

Sohn, H., Dzwonczyk M. , Straser E.G., Kiremidjian A.S., Law K.H., and Meng T. (1999) "An Experimental Study of Temperature Effects on Modal Parameters of the Alamosa Canyon Bridge," *Earthquake Engineering and Structural Dynamics*, Vol. 28 pp. 879-897.

Soong, T.T. and Spencer, B.F., Jr. (2002), Supplemental Energy Dissipation: State-of-the Art and State-of-the-Practice, *Engineering Structures*, Vol. 24 pp. 243-259.

Sigaher, A.N. and Constantinou, M.C. (2003). "Scissor-Jack-Damper Energy Dissipation System," *Earthquake Spectra*, Vol. 19.1 pp. 133-158.

Spencer, B.F., Jr. and Nagarajaiah, S. (2003). "State of the Art of Structural Control," *Journal of Structural Engineering,* Vol. July 2003 pp. 845-856.

Spencer, B.F., Jr. and Sain, M.K. (1997). "Controlling Buildings: A New Frontier in Feedback," *IEEE Control Systems Magazine*, Vol. 17.6 pp. 19-35.

U.S. Department of Transportation, Federal Highway Administration (2001) "Highway Bridge Inspection: State-of-the-Practice Survey," FHWA-RD-01-033.

Xu Y.L. and Chen B. (2007). "Integrated Vibration Control and Health Monitoring of Building Structures using Semi-Active Friction Dampers: Part I - Methodology." *Engineering Structures.*

Zeng, H., Kuehn, J., Song, G., Sun, J., and Stalford, H. (2000). "A Semi-Active Controller for the Vibration Absorber on the I-35 Walnut Creek Bridge," *American Control Conference Proceedings*, Chicago, IL, June, 2000.